Am J Cancer Res 2022;12(1):68-90
www.ajcr.us /ISSN:2156-6976/ajcr0140193

Original Article

Differential expression profile of CXC-receptor-2 ligands as potential biomarkers in pancreatic ductal adenocarcinoma

Sugandha Saxena[1], Caitlin Molczyk[1], Abhilasha Purohit[1], Evie Ehrhorn[1], Paran Goel[1], Dipakkumar R Prajapati[1], Pranita Atri[2], Sukhwinder Kaur[2], Paul M Grandgenett[3], Michael A Hollingsworth[3], Surinder K Batra[2], Rakesh K Singh[1]

[1]Department of Pathology and Microbiology, 985950 Nebraska Medical Center, Omaha, NE 68198-5900, USA; [2]Department of Biochemistry and Molecular Biology, University of Nebraska Medical Center, Omaha, NE 68198-5845, USA; [3]Eppley Institute for Research in Cancer and Allied Diseases, Fred & Pamela Buffett Cancer Center, University of Nebraska Medical Center, Omaha, NE 68198, USA

Received October 29, 2021; Accepted December 3, 2021; Epub January 15, 2022; Published January 30, 2022

Abstract: The discovery of early detection markers of pancreatic cancer (PC) disease is highly warranted. We analyzed the expression profile of different CXC-receptor-2 (CXCR2) ligands in PC cases for the potential of biomarker candidates. Analysis of different PDAC microarray datasets with matched normal and pancreatic tumor samples and next-generation sequenced transcriptomics data using an online portal showed significantly high expression of CXCL-1, 3, 5, 6, 8 in the tumors of PC patients. High CXCL5 expression was correlated to poor PC patient survival. Interestingly, mRNA and protein expression analysis of human PC cell lines showed higher CXCL2, 3, and 5 expressions in cell lines derived from metastatic sites than primary tumors. Furthermore, we utilized immunohistochemistry (IHC) to evaluate the expression of CXCR2 ligands in the human PC tumors and observed positive staining for CXCL1, 3, and 8 with a higher average IHC composite score of CXCL3 in the PC tissue specimens than the normal pancreas. We also observed an increase in the expression of mouse CXCL1, 3, and 5 in the pre-cancerous lesions of tumors and metastasis tissues derived from the PDX-cre-LSL-Kras^{G12D} mouse model. Together, our data suggest that different CXCR2 ligands show the potential of being utilized as a diagnostic biomarker in PC patients.

Keywords: CXCR2, CXCL1, CXCL3, CXCL5, CXCL8, pancreatic cancer

Introduction

Pancreatic Cancer (PC) remains a challenging disease due to its late clinical presentation with metastatic dissemination at the time of diagnosis [1-3]. Other factors that affect this disease's outcome are the limited number of patients that qualify for surgical resection, the inadequacy of the currently available detection techniques, and less effective chemotherapeutic treatments for combating the disease. Thus, even though PC is less common in occurrence, the disease has a higher mortality rate than other cancer types [4]. With all the above mentioned factors, improving this disease's clinical outcome necessitates research focusing on early detection markers. In the current study, we present an effort to identify the potential of the CXCR2 receptor's inflammatory chemokines as biomarkers during PC's inception and progression.

Chemokines, the members of the supergene family of chemotactic cytokines, are a horde of low molecular weight inflammatory cytokines that recruit leukocytes to an inflammatory area [5]. There are four subfamilies of chemokines based on the location of N-terminal cysteine residues: CXC, CC, CX3C, and XC [6]. The members of these four families of chemokines differ in their structure, the chromosomal location of their genes, and the target cell's response [7]. After the initial characterization of chemokines as immune cell recruiters, the plethora of recent research highlights their pivotal role in cancer biology by affecting both the tumor cells

and tumor microenvironment. Chemokines influence different cancer cell properties such as tumor growth and proliferation, epithelial to mesenchymal transition, cancer stem cell properties, and chemotherapy resistance, and can modify the tumor microenvironment through leukocyte recruitment, stromal interactions, angiogenesis, and creating metastatic niches [8].

The CXC subfamily or α-chemokine comprises seventeen members. Some family members have a characteristic Glu-Leu-Arg (ELR) motif located at the N-terminus before the first cysteine amino acid residue [9]. This ELR motif is associated with the chemokine's angiogenic nature [10]. Thus, the CXC family can further divide into two groups based on the presence or absence of an ELR motif. The ELR+ chemokines are, in general, promoters of angiogenesis, play a role in endothelial cell chemotaxis, and neutrophils recruitment, known for their synthesis and storage of angiogenic molecules [11, 12]. On the other hand, ELR$^-$ members are usually angiogenesis inhibitors [10, 13] with T and B cell recruitment properties.

CXC-receptor 2 (CXCR2) ligands (CXCL1-3, 5-8) are all ELR+ angiogenic chemokines that assist in delivering oxygen and nutrients to the tumor to constitute a vascular network, thereby enhancing the invasiveness of tumors. Our current study focuses on different methods to examine their expression profile for evaluation as potential biomarker candidates. CXCR2 plays a critical role in different cancers, such as lung cancer [14, 15], breast cancer [16-21], clear-cell renal cell carcinoma [22], hepatocellular carcinoma [23], melanoma [24-27], and pancreatic ductal carcinoma [28-30]. Moreover, recent studies suggest that CXCR2 could be considered a target for PC and metastasis treatment [31, 32]. Varied studies in different tumor types have drawn a consensus regarding the role of CXCR2 and the ligands. However, our study attempts to analyze the prognosis value of CXCR2 ligands in PC comprehensively.

We utilized different approaches for the evaluation of the biomarker potential of CXCR2 ligands. Such as online Oncomine, Michigan Portal for the Analysis of NGS data (MiPanda), and Gene Expression Profiling Interactive Analysis (GEPIA) portals with microarray and analyzed next-generation sequenced transcriptomics data. Similarly, we utilized the Badea cohort (GSE15471) [33], Pei Pancreas (GSE16515) [34], and Zhang cohort (GSE28735) [35] containing matched pancreatic tumors with corresponding matched normal samples. We also performed CXCR2 ligands expression analysis in nine different human PC cell lines. We evaluated the ligand expression pattern in pancreatic tissues and metastatic liver derived from the disease progression mouse model of PDX-cre-LSL-KRAS^{G12D} and the human PC tissue specimens. In conclusion, our analysis suggests that among different CXCR2 ligands, CXCL5 shows the potential of being used as a biomarker in PC patients.

Material and methods

Online portals

Oncomine analysis: Oncomine (www.oncomine.org) is a public cancer microarray database with a web-based data-mining platform designed to facilitate gene expression analyses for various tumors [36]. We utilized the Badea Pancreas (39 normal pancreas and 39 PC samples) and Pei Pancreas databases (16 normal pancreas and 36 PC samples) in the PC Oncomine database to analyze the expression level of the CXCR2 receptor and ligands. We used a *P*-value of 0.0001, a fold change of 2, and the top 10% genes as thresholds for our analysis. Oncomine automatically generates bar-graphs of expression data based on the input gene from the two utilized databases.

GEPIA analysis: GEPIA (http://gepia.cancer-pku.cn/) is an online web-based data-mining portal that integrates gene expression data from (TCGA) and the Genotype-Tissue Expression (GTEx) project [37]. We utilized the GEPIA database to explore CXCR2 receptor and ligands' gene expression as a differential function of normal (171 samples) and pancreatic tumor (179 samples), different pathological stages according to the TCGA clinical annotation, similar gene detection, and patient survival analysis. We plotted logarithmic expression of TPM (log2 (TPM+1)) transformed expression data. GEPIA automatically generates different plots such as a box or violin plot based on the different gene input.

MiPanda analysis: MiPanda (http://mipanda.org) is a public online portal that provides

Table 1. Details of the GEO datasets utilized in the study

	GEO Accession	Last name of the first author	Normal Samples	Tumor Samples	Matched	Number of genes
1	GSE15471	Badea	36	36	36	54775
2	GSE 16515	Pei	16	36	16	54613
3	GSE 28735	Zhang	45	45	45	28869

access to large-scale computational analysis of high-throughput RNA sequencing samples [38]. We utilized this portal to access PC-specific CXCR2 receptor and ligands gene expression profiles across numerous normal pancreas, cancer tissues and, metastasis. Currently, the portal contains a combined 417 RNA sequencing samples of normal pancreas and tumor tissue. Our current study has modified the automatically generated graph from the portal with the expression of gene plotted in logarithmic TPM across normal pancreas, primary PC samples, and metastases.

OncoLnc analysis: OncoLnc (http://www.oncolnc.org.) is an online tool that explores survival correlations based on mRNAs, miRNAs, or long non-coding RNAs (lncRNAs) expression data for different genes. OncoLnc retrieves RNA-sequencing expression for mRNAs and miRNAs from TCGA and lncRNA expression from MiTranscriptome beta. We utilized precomputed survival analyses generated as Kaplan-Meier plots for gene expression of CXCR2 receptor and ligands in PC patients' analyses [39].

Microarray-based gene-expression profiles of matched pairs of PDAC tumor and adjacent non-tumor tissues

We downloaded raw data of the following microarray gene expression profiles-GSE15471 [33], GSE16515 [34], and GSE28735 [35] from the GEO database, NCBI gene expression, and hybridization array data repository. We analyzed the obtained raw data using Wilcoxon analysis in GraphPad Prism 8.0 software (San Diego, CA). **Table 1** contains details of the three datasets utilized for matched PDAC tumor and adjacent non-tumor tissues.

Cell culture

We obtained the human PC cell line T3M-4 as a generous gift from Dr. Hollingworth's laboratory at the University of Nebraska Medical Center (UNMC), Omaha, Nebraska. Similarly, we obtained human PC cell lines such as CD18-HPAF, Panc-1, MiaPaCa-2, Capan-1, and BxPC-3 as generous gifts from Dr. Batra's laboratory, UNMC Omaha, Nebraska. We received human L3.3 and L3.6pl [40] as generous gift from Dr. I.J. Fidler in the University of Texas M.D. Anderson Cancer Center. We also utilized a model of immortalized human pancreatic duct-derived cell lines, with or without exogenous expression of $KRAS^{(G12D)}$-hTERT-HPNE (HPNE) and hTERT-HPNE-$KRAS^{(G12D)}$ (HPNE-KRAS) as described previously [41]. We purchased PC cell line AsPC-1 from American Type Culture Collection (Manassas, VA). We have described cell culture and maintenance previously [42]. In brief, we maintained cell lines such as T3M-4, CD18-HPAF, MiaPaCa-2, and Panc-1 in Dulbecco's Modified Eagle Medium (DMEM) (Hyclone Laboratories, Logan, UT) supplemented with 5% fetal bovine serum (FBS) (Sigma-Aldrich, St. Louis, MO), 1% of 100X Minimum Essential Medium (MEM) vitamin solution (Mediatech, Herdon, VA), 1% of 200 mM L-glutamine (Mediatech) and 8 mg/mL of gentamycin (Invitrogen, Carlsbad, CA). We cultured AsPC-1 and BxPC-3 using Roswell Park Memorial Institute medium (Sigma-Aldrich) supplemented with 5% FBS (Sigma-Aldrich), 1% of 200 mM L-glutamine (Mediatech), and 8 mg/mL gentamycin (Invitrogen). We cultured Capan-1 cells in Iscove's Modified Dulbecco's Medium (IMDM) (Sigma-Aldrich) with 20% FBS (Sigma-Aldrich), 1% of 100X MEM vitamin solution (Mediatech), 1% of 200 mM L-glutamine (Mediatech) and 8 mg/mL gentamycin (Invitrogen). Lastly, we maintained HPNE and HPNE-Kras in unique media consisting of three parts DMEM (HyClone) and one part M3:5 growth medium (Incell, San Antonio, TX) supplemented with 5% FBS, (Sigma-Aldrich), 1% of 100X MEM vitamin solution (Mediatech), 1% of 200 mM L-glutamine (Mediatech) and 8 mg/mL of gentamycin (Invitrogen).

RNA extraction and analysis

We seeded different cell lines at a density of 1×10^6 in a 100 mm dish overnight. We isolated total cellular RNA from these different cell lines the following day using TRIzol® reagent

Table 2. List of human primers used for the study

S. No	Gene	Melting Temp	Forward Primer	Reverse Primer
1	HPRT	58°C	GTTGGATACAGGCCAGACTTTCTTG	GATTCAACTTGCGCTCATCTTAGGC
2	CXCR1	59°C	TGGGAAATGACACAGCAAAA	AGTGTACGCAGGGTGAATCC
3	CXCR2	58°C	ACTTTTCCGAAGGACCGTCT	GTAACAGCATCCGCCAGTTT
4	CXCL1	59°C	ATTCACCCCAAGAACATCCA	CACCAGTGAGCTTCCTCCTC
5	CXCL2	59°C	GCAGGGAATTCACCTCAAGA	AGCTTCCTCCTTCCTTCTGG
6	CXCL3	59°C	GCAGGGAATTCACCTCAAGA	GGTGCTCCCCTTGTTCAGTA
7	CXCL5	57°C	AGCTGCGTTGCGTTTGTTTAC	TGGCGAACACTTGCAGATTAC
8	CXCL6	58°C	GAATTTCCCCAGCATCCCAAAG	TGCCTTCTGCACTCCCTTTATC
9	CXCL7	58°C	ACTTGTAGGCAGCAACTCACC	GGTGGAGAAGGCTGAGCTAG
10	CXCL8	59°C	ACATACTCCAAACCTTTCCACCC	CAACCCTCTGCACCCAGTTTTC

(Invitrogen, Carlsbad, CA) as described previously [43]. We resuspended the obtained RNA in 20 µl of diethylpyrocarbonate (DEPC) containing water, quantified using absorbance at 260 nm, and checked the quality of the RNA. We synthesized cDNA using two µg of the obtained RNA for a twenty µl reaction using High-Capacity cDNA Reverse Transcription Kit (applied biosystems, Thermo Fischer Scientific, Carlsbad, CA). We prepared qRT-PCR reactions using PowerUp™ SYBR™ Green Master Mix (Thermo Fisher), cDNA, gene-specific primers (**Table 1**), and nuclease-free water. We analyzed the results using Thermo Fisher Connect (Thermo Fisher). We calculated the mean Ct values of the target genes and normalized the obtained values to mean Ct values of the endogenous control, HPRT; [-ΔCt = Ct (HPRT) - Ct (target gene)]. Furthermore, we performed a melting curve analysis to check the specificity of the amplified products. The details of the sequence of gene-specific primers are in **Table 2**.

Protein isolation, quantification, and immunoblotting

We seeded different cell lines at a density of 1×10^6 in a 100 mm dish overnight. The following day we washed the cells thrice with Phosphate Buffer Saline (PBS) and added serum-free media. Furthermore, we incubated these cells for 72 hours before isolating proteins. We isolated and quantified proteins for immunoblotting as described previously (plexin-B3). In brief, we lysed the cells using Membrane Lysis Buffer (M-PER®, Pierce, Rockford, IL) containing protease inhibitors (Complete mini, Roche Diagnostics, Mannheim, Germany). We utilized a BCA kit (Pierce™ BCA and Protein Assay Kit (Thermo Scientific, Rockford, IL) for protein quantitation and followed the protocol as described by the manufacturer. We separated the denatured proteins on a 10% SDS-PAGE and transferred the proteins to a 0.45 µm PVDF membrane (Millipore, Billerica, MA). Next, we blocked the membrane with 3% Bovine Serum Albumin (BSA, Sigma) in 0.1% Tween containing Tris Buffer Saline (TBST) and incubated the membrane with the respective primary antibody (**Table 3**) at 4°C overnight. The following day, we incubated the membrane with secondary horseradish peroxidase antibody (mouse (Sigma)), 1:5000; rabbit (Thermo Scientific), 1:5000 and finally developed the blots using the Luminata™ Forte (Millipore) on Molecular Imager® Gel Doc™ XR System (BIO-RAD) using Image Lab version 5.2.1.

Enzyme-linked immunosorbent assay (ELISA)

We seeded different cell lines at a density of 1×10^6 in a 100 mm dish overnight and followed the protocol described in the above section. After incubating these cells in serum-free media for 72 hours, we collected the supernatants from these cells. According to the manufacturer's protocol, we performed an ELISA assay for human CXCL1 (DY275) and CXCL5 (DY254) using a duo set sandwich ELISA assay kit (R&D Systems, Minneapolis, MN). Similarly, according to the manufacturer's protocol, we utilized monoclonal CXCL8 antibody (M-801-E, Endogen, Woburn, MA) for coating and biotin-labeled detecting antibody (M-802-B, Endogen) for the development of the assay.

Also, serum levels of CXCL1, CXCL5, and CXCL8 from human patient samples were quantified using Human duo set sandwich ELISA assay as per manufactures instructions (R&D Systems).

Table 3. List of antibodies used for IHC and immunoblotting

Species reactivity in this paper	Antibody	Supplier	Catalog number	Host species	Dilution
Mouse	CXCR2	A kind gift from Dr. Strieter		Goat	1:1000
Mouse/Human	Gro alpha	Abcam	ab86436	Rabbit	1:500
Mouse/Human	CXCL3	Bioss	bs-2547R	Rabbit	1:500
Mouse	CXCL5	Cloud-clone corp.	PAA860Mu01	Rabbit	1:100
Human	CXCR2	Abcam	ab14935	Rabbit	IHC-1:200, WB: 1:500
Human	CXCL8	Pierce Endogen	P801	Rabbit	1:200

The serum samples were obtained under the Institutional Review Boards (IRB) of the University of Nebraska Medical Center (UNMC) (IRB number 209-00). Consent was obtained from all patients and controls, and inclusion criteria were any adult patient (age ≥18 years) with histologically proven PC. Chronic pancreatitis (CP) was defined based on CT scan findings of calcifications, abnormal pancreatogram, or secretin stimulation test. The 96-well plates were coated with anti- Human CXCL1/5/8 capture antibodies (4 µg/ml concentration) in PBS overnight at room temperature (RT). After three washes with wash buffer PBS containing 0.05% Tween 20 (PBS-T) using a plate washer (BioTek, ELx50, BioTek, Winooski, VT), plates were blocked with 3% BSA (Probumin, Millipore) for two hours at RT followed by three washings with PBS-T. The linear range of standards (ranges from 12,000-11.7 pg/ml) and appropriate serum dilution (1:5 dilutions) in 1% BSA were added in duplicates, and plates were incubated overnight at 4°C. After three washes with wash buffer, standards and samples were incubated with biotinylated detection antibodies in 1% BSA for 2 hrs at RT. After washing thrice, the streptavidin-HRP was added onto plated for 20 minutes at RT. Signal was developed using TMB substrate (Millipore), and the final reaction was stopped with a stop solution (2N H_2SO_4). Plates were read at 450 nm, and concentrations in serum samples were interpolated using logistic-4 regression on the FindGraph software (Vancouver, BC).

Immunohistochemistry

We have previously described the method of IHC in detail in [44]. In brief, we deparaffinized 4 µm thick, formalin-fixed, paraffin-embedded sections using the gradient of alcohol and xylene. We performed antigen retrieval using sodium citrate buffer (pH=6.0) and microwaving for 10 minutes following deparaffinization. Next, we blocked endogenous peroxidase by incubating it with 3% hydrogen peroxide in methanol for 30 minutes. We probed slides with appropriate primary antibodies after blocking, as detailed in **Table 3**, overnight at 4°C. The following day, we washed the slides using PBS and incubated them for an hour with appropriate secondary antibodies. We detected immunoreactivity using the ABC Elite Kit (Vector Laboratories, Burlingame, CA) and 3, 3 diaminobenzidine substrate kit (Vector Laboratories) as per the manufacturer protocols, respectively. Furthermore, we counterstained the nuclei with hematoxylin.

IHC score was calculated according to the following criteria: Percentage of positive cells on the slides was as follows: 0 (negative), 1 (1-25% of cells positive), 2 (>25-50% of cells positive), 3 (>50-75% of cells positive), and 4 (>75-100%). Furthermore, the intensity was designated as weak (1 point), moderate (2 points), and strong (3 points). The IHC composite score was calculated by multiplying the extent of positive cells with intensity (maximum score of 12). Average scores from two independent observers were reported.

Mouse model of PC disease progression and metastasis specimens

We utilized tissue sections of primary pancreatic tumors and liver metastasis of the PDX-cre-LSL-Kras$^{(G12D)}$ (KC) mice [45]. We obtained pancreatic tumors of KC mice from different time points/ages (10, 25, and 50 weeks) and metastatic liver sites of KC mice at the 50-week time point for our study. Five tumor sections of each stage were used to evaluate the expression of different ligands. The Tissue science facility at the University of Nebraska Medical Center (UNMC) processed, paraffin-embedded, and sectioned the collected tissue specimens.

Human PC patient specimens

We obtained Tissue Microarray (TMA) slides from the UNMC rapid autopsy program. The Institutional Review Board of the UNMC has approved the rapid autopsy program (UNMC IRB 091-01). Constructed from paraffin blocks, TMAs contained pancreatic tumor cores, non-cancerous pancreas, and control specimens of gastric tissue.

The serum samples were obtained under the Institutional Review Boards (IRB) of the University of Nebraska Medical Center (UNMC) (IRB number 209-00). Consent was obtained from all patients and controls before enrollment into the study. Inclusion criteria were any adult patient (age ≥18 years) with histologically proven PC. Chronic pancreatitis (CP) was defined based on CT scan findings of calcifications, abnormal pancreatogram, or secretin stimulation test.

Results

Oncomine datasets demonstrate higher expression of CXCL3, CXCL5, and CXCL8 in pancreatic tumors in comparison with normal pancreas

We utilized different online portals to examine the expression of CXCR2 ligands in PC patients. First, we examined Pei and Badea PC datasets present in the Oncomine database [36], which contained a differential gene expression analysis of PC tumors and the normal pancreas. We screened for CXCR2 ligands (**Figure 1A-F**) and observed significantly higher expression of CXCL3 (**Figure 1A**, **1D**), CXCL5 (**Figure 1B**, **1E**), and CXCL8 (**Figure 1C**, **1F**) in pancreatic tumors in comparison with normal pancreas. CXCL3 showed five-fold higher expression in pancreatic tumors (*P*-value 3.8E-7, t-tests-5.806 with overexpression (OE) gene rank of 433). It was among the top 3% of the differentially expressed genes in the Pei dataset (**Figure 1A**). Similarly, CXCL3 showed nearly four-fold higher expression in pancreatic tumors (*P*-value 1.19E-8, t-tests-6.423 with OE gene rank of 1428). It was among the top 8% of the differentially expressed genes in the Badea dataset (**Figure 1D**). On the other hand, CXCL5 nearly showed 13 fold higher expression (*P*-value 5.58E-9, t-tests: 6.828, OE gene rank of 16) and was among the top 1% of the differentially expressed genes in the Pei dataset (**Figure 1B**). Uniformly, CXCL5 showed an 8.6 fold higher expression in pancreatic tumors *(P*-value 3.37E-13, t-tests-8.638, OE gene rank of 211) and was among the top 2% of the differentially expressed gene genes in the Badea dataset (**Figure 1E**). Lastly, CXCL8 showed eight-fold higher expression (*P*-value 3.51E-6, t-tests: 5.473, OE gene rank of 719) and was among the top 4% of the differentially expressed genes in the Pei dataset (**Figure 1C**). Likely, CXCL8 showed a 9.8 fold higher expression in pancreatic tumors (*P*-value 9.92E-12, t-tests-7.971, OE gene rank of 380) and was among the top 2% of the differentially expressed genes in the Badea dataset (**Figure 1F**).

MiPanda database demonstrate higher expression of CXCL1, CXCL3, CXCL5, CXCL6, and CXCL8 in pancreatic tumors and metastasis in comparison with normal pancreas

We examined the expression of CXCR2 ligands in normal pancreatic tissues, PC tissues, and metastasis at the MiPanda database [38]. Expression of CXCL1, CXCL3, CXCL5, CXCL6, and CXCL8 was significantly higher, whereas CXCL2 was significantly lower in PC tissues and metastasis in comparison with normal tissues (**Figure 1G-L**). The median value of logarithmic CXCR2 ligands transcripts per million (TPM) expression for PC tumor, metastases, and normal pancreas and are listed in **Table 4**. CXCL5 expression showed the highest fold change difference of 197.67 in pancreatic tumors compared to the normal pancreas (**Figure 1J**), followed by CXCL8 (107.46 fold change) (**Figure 1L**), CXCL3 (95.92 fold change) (**Figure 1I**), CXCL6 (42.46 fold change) (**Figure 1K**) and CXCL1 (26.92 fold change) (**Figure 1G**). Apart from the highest fold change difference of CXCL5, the range of CXCL5 expression in the normal pancreas was narrow. All the expression values were lower than the median of CXCL5 expression in pancreatic tumors.

We utilized the GEPIA database [37] to validate further the expression of CXCR2 ligands in normal pancreas and pancreatic tumor tissues (**Figure 1M-R**). Similar to MiPanda, CXCL1 (**Figure 1M**), CXCL3 (**Figure 1O**), CXCL5 (**Figure 1P**), CXCL6 (**Figure 1Q**), and CXCL8 (**Figure 1R**), showed significantly higher logarithmic expression TPM+1 ($P<0.01$) whereas CXCL2 (**Figure 1N**) showed a non-significant trend of lower expression in PC tissues than normal tissues.

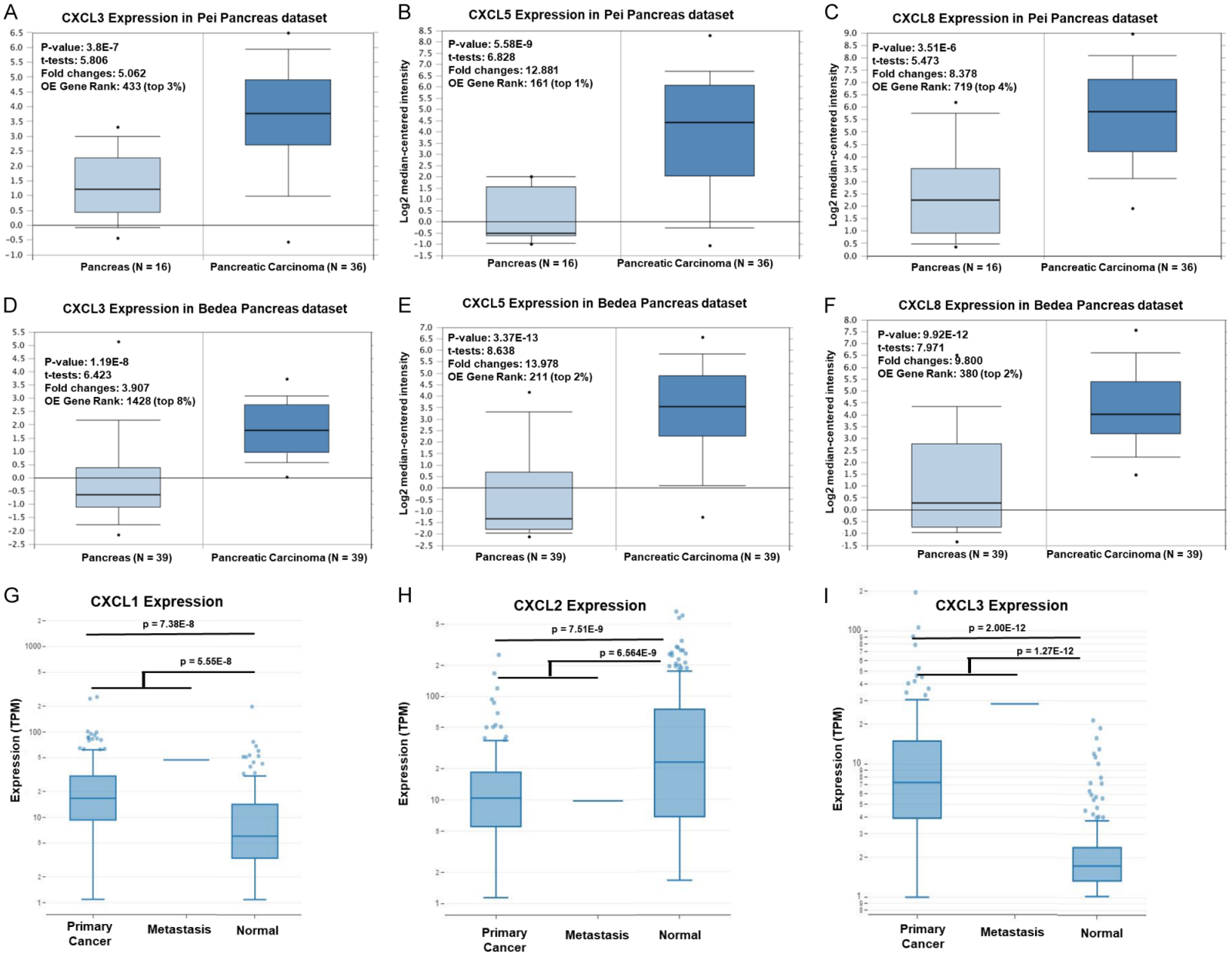
A
CXCL3 Expression in Pei Pancreas dataset
P-value: 3.8E-7
t-tests: 5.806
Fold changes: 5.062
OE Gene Rank: 433 (top 3%)
Pancreas (N = 16)
Pancreatic Carcinoma (N = 36)
B
CXCL5 Expression in Pei Pancreas dataset
P-value: 5.58E-9
t-tests: 6.828
Fold changes: 12.881
OE Gene Rank: 161 (top 1%)
Log2 median-centered intensity
Pancreas (N = 16)
Pancreatic Carcinoma (N = 36)
C
CXCL8 Expression in Pei Pancreas dataset
P-value: 3.51E-6
t-tests: 5.473
Fold changes: 8.378
OE Gene Rank: 719 (top 4%)
Log2 median-centered intensity
Pancreas (N = 16)
Pancreatic Carcinoma (N = 36)
D
CXCL3 Expression in Bedea Pancreas dataset
P-value: 1.19E-8
t-tests: 6.423
Fold changes: 3.907
OE Gene Rank: 1428 (top 8%)
Pancreas (N = 39)
Pancreatic Carcinoma (N = 39)
E
CXCL5 Expression in Bedea Pancreas dataset
P-value: 3.37E-13
t-tests: 8.638
Fold changes: 13.978
OE Gene Rank: 211 (top 2%)
Log2 median-centered intensity
Pancreas (N = 39)
Pancreatic Carcinoma (N = 39)
F
CXCL8 Expression in Bedea Pancreas dataset
P-value: 9.92E-12
t-tests: 7.971
Fold changes: 9.800
OE Gene Rank: 380 (top 2%)
Log2 median-centered intensity
Pancreas (N = 39)
Pancreatic Carcinoma (N = 39)
G
CXCL1 Expression
p = 7.38E-8
p = 5.55E-8
Expression (TPM)
Primary Cancer
Metastasis
Normal
H
CXCL2 Expression
p = 7.51E-9
p = 6.564E-9
Expression (TPM)
Primary Cancer
Metastasis
Normal
I
CXCL3 Expression
p = 2.00E-12
p = 1.27E-12
Expression (TPM)
Primary Cancer
Metastasis
Normal

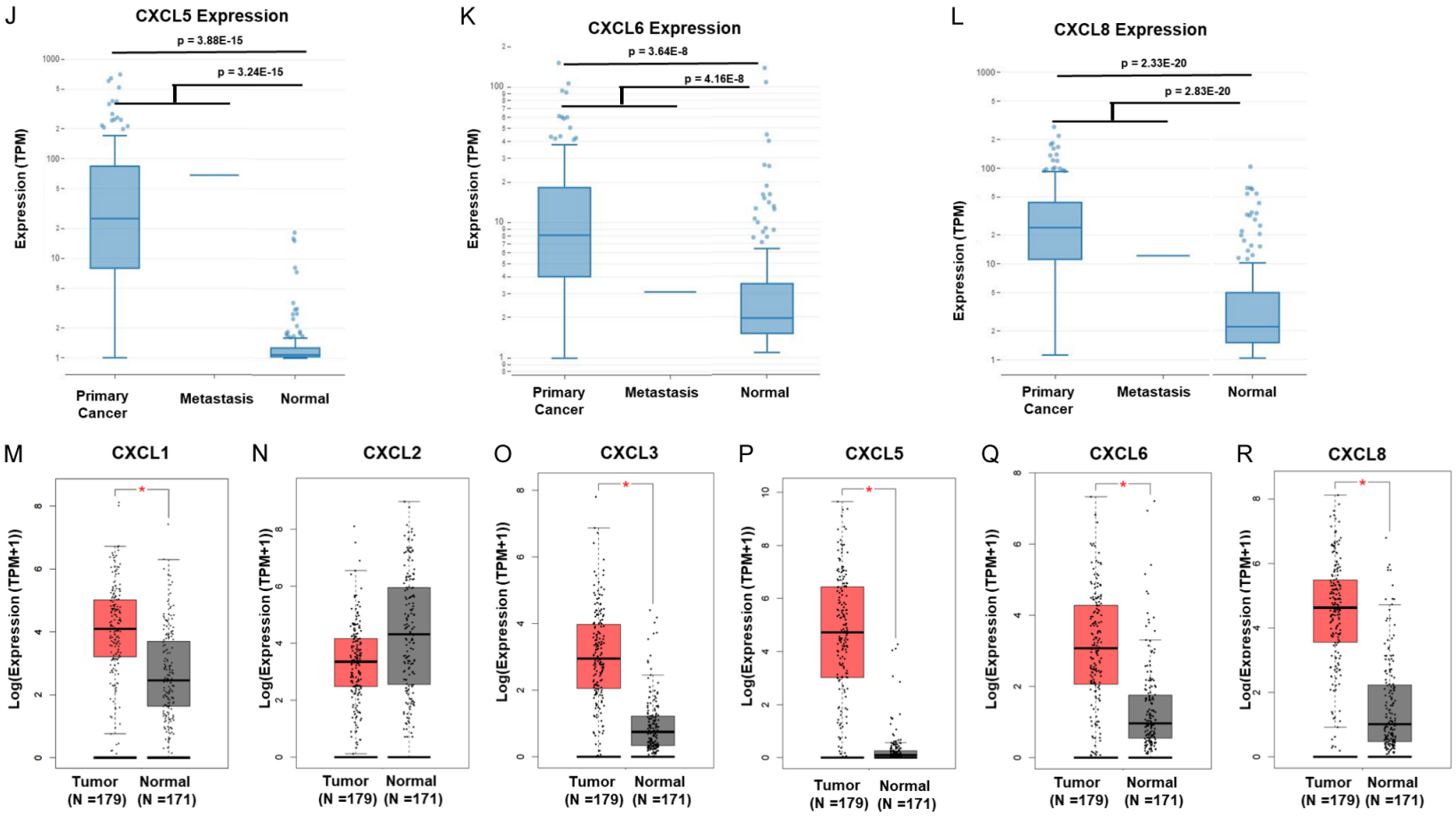

Figure 1. Different online portals demonstrate significantly high CXCR2 ligands expression in patients with PC. (A-C) The differential CXCR2 ligands expression analysis was performed on the Pei PC microarray dataset present in the Oncomine database. Box plot shows higher expression of CXCL3 (A, P=3.8E-7), CXCL5 (B, P=5.58E-9) and CXCL8 (C, P=3.51E-6) in PC patients than normal pancreas. (D-F) The differential CXCR2 ligands expression analysis was carried out on the Badea PC microarray dataset present in the Oncomine database. Box plot graph showing higher expression of CXCL3 (D, P=1.19E08), CXCL5 (E, P=3.37E-13) and CXCL8 (F, P=9.92E-12) in PC patients than normal pancreas. (G-L) In the MiPanda online platform, box plot demonstrates significantly high logarithmic TPM expression of CXCL1 (G, P=7.38E-8), CXCL3 (I, P=2.00E-12), CXCL5 (J, P=3.88E-15), CXCL6 (K, P=3.64E-8) and CXCL8 (L, P=2.33E-20) whereas low CXCL2 (H, P=7.51E-9) expression in pancreatic tumors and metastasis in comparison with normal pancreas. (M-R) In the GEPIA online platform, box plot demonstrates significantly high logarithmic TPM+1 expression of CXCL1 (M), CXCL3 (O), CXCL5 (P), CXCL6 (Q), and CXCL8 (R), whereas non-significant low CXCL2 (N) expression in pancreatic tumors and metastasis in comparison with the normal pancreas (P<0.01). Red indicates pancreatic tumor tissue; gray indicates normal pancreatic tissue.

Table 4. CXCR2 ligands expression in pancreatic tumors

		Normal	Cancer	Metastasis	*P*-value (primary cancer vs Normal)	*P*-value (primary cancer, metastasis vs Normal)
1	CXCL1	6.036	16.647	46.941	7.38E-8	5.55e-8
2	CXCL2	22.913	10.416	9.794	7.51E-9	6.64E-9
3	CXCL3	1.734	7.293	28.412	2.00E-12	1.27E-12
4	CXCL5	1.087	25.039	68.22	3.88E-15	3.24E-15
5	CXCL6	1.961	8.124	3.096	3.64E-8	4.16E-8
6	CXCL8	2.203	24.0325	12.18	2.33E-20	2.83E-20

MiPanda database demonstrates higher expression of CXCL1, CXCL3, CXCL5, CXCL6, and CXCL8 in pancreatic tumors compared to normal pancreas.

Matched pancreatic tumors and corresponding normal pancreas sample analysis from different gene expression omnibus (GEO) datasets demonstrate high CXCR2 ligand expression in PC patients

We downloaded raw data of microarray gene expression profile of CXCR2, different CXCR2 ligands, and CXCR1 from Badea-GSE15471 [33], Pei-GSE16515 [34], and Zhang-GSE28735 [35] datasets present in the (GEO). We only analyzed expression datasets of the patient having both matched pancreatic tumors and corresponding normal pancreas samples from these raw data. The Badea-GSE15471 dataset contained probes for all CXCR2 ligand samples as well as CXCR1 and CXCR2 (**Figure 2A-H**). With a sample size of 34 patients, analyzing the Badea dataset showed more patients with a higher CXCL1 (*P*-value =4E-4) (**Figure 2A**), CXCL3 (*P*-value <1E-4) (**Figure 2C**), CXCL5 (*P*-value <1E-4) (**Figute 2D**), CXCL6 (*P*-value <1E-4) (**Figure 2E**), and CXCL8 (*P*-value <1E-4) (**Figure 2F**) in the matched tumor than adjacent normal samples, whereas CXCL2 and CXCR1 showed more patients with a trend of lower expression in the matched tumor than adjacent normal samples. On the other hand, the trend of CXCR2 expression was not conclusive. Pei-GSE16515, with matched samples of 16 patients, also contained expression profiles for CXCR2, all CXCR2 ligand samples, and CXCR1. Analyses of the Pei dataset showed a trend indicating a greater number of patients with significantly higher amounts of CXCL3 (*P*-value =8E-40) (**Figure 2I**), CXCL5 (*P*-value <3E-4) (**Figure 2J**), CXCL7 (*P*-value =2.5E-2) (**Figure 2K**), and CXCL8 (*P*-value =1E-3) (**Figure 2L**) in the matched tumor in comparison to the adjacent normal samples. Lastly, the Zhang-GSE28735 dataset containing matched samples of 45 patients contained limited-expression probes for CXC family ligands and receptors; however, CXCL3 (*P*-value =5.3E-3) (**Figure 2M**), CXCL5 (*P*-value <1E-4) (**Figure 2N**), and CXCL8 (*P*-value =4.1E-3) (**Figure 2O**) showed a significant trend of higher expression while CXCR1 (*P*-value =3.2E-2) (**Figure 2P**) showed a trend of significant lower expression in pancreatic tumors compared to their respected matched normal samples.

GEPIA plots of CXCR2 ligand expression are significantly different across PC pathological stages

GEPIA can plot gene expression by pathological stages based on The Cancer Genome Atlas (TCGA) clinical annotation. We observed significant differences of CXCL1 (F value =2.91, Pr(>F) =3.61E-2) (**Figure 3A**), CXCL3 (F value =3.97, Pr(>F) =1.15E-2) (**Figure 3B**), CXCL5 (F value =5.84, Pr(>F) =8.05E-4) (**Figure 3C**) and CXCL8 (F value =3.61, Pr(>F) =1.45E-2) (**Figure 3D**) expression across different PC pathological stages. All the four ligands CXCL1, CXCL3, CXCL5, and CXCL8, showed a higher median and narrow range of expression in the later stages of the disease. Among the four ligands showing significant association with the pathological stages, CXCL5 (**Figure 3C**) expression demonstrated the most direct and logical pattern of increase in expression. However, we do acknowledge that less than 3% of TCGA data represents stage IV. Hence the analysis of the dataset with pathological stages is not robust. Also, CXCL5 expression based on mRNAs showed a significant correlation with the survival of PC patients generated as Kaplan-Meier plots from the OncoLnc tool (*P*-value =9.31E-3) (**Figure 3E**). We selected the 25th percentile suggesting we compared upper quartile data

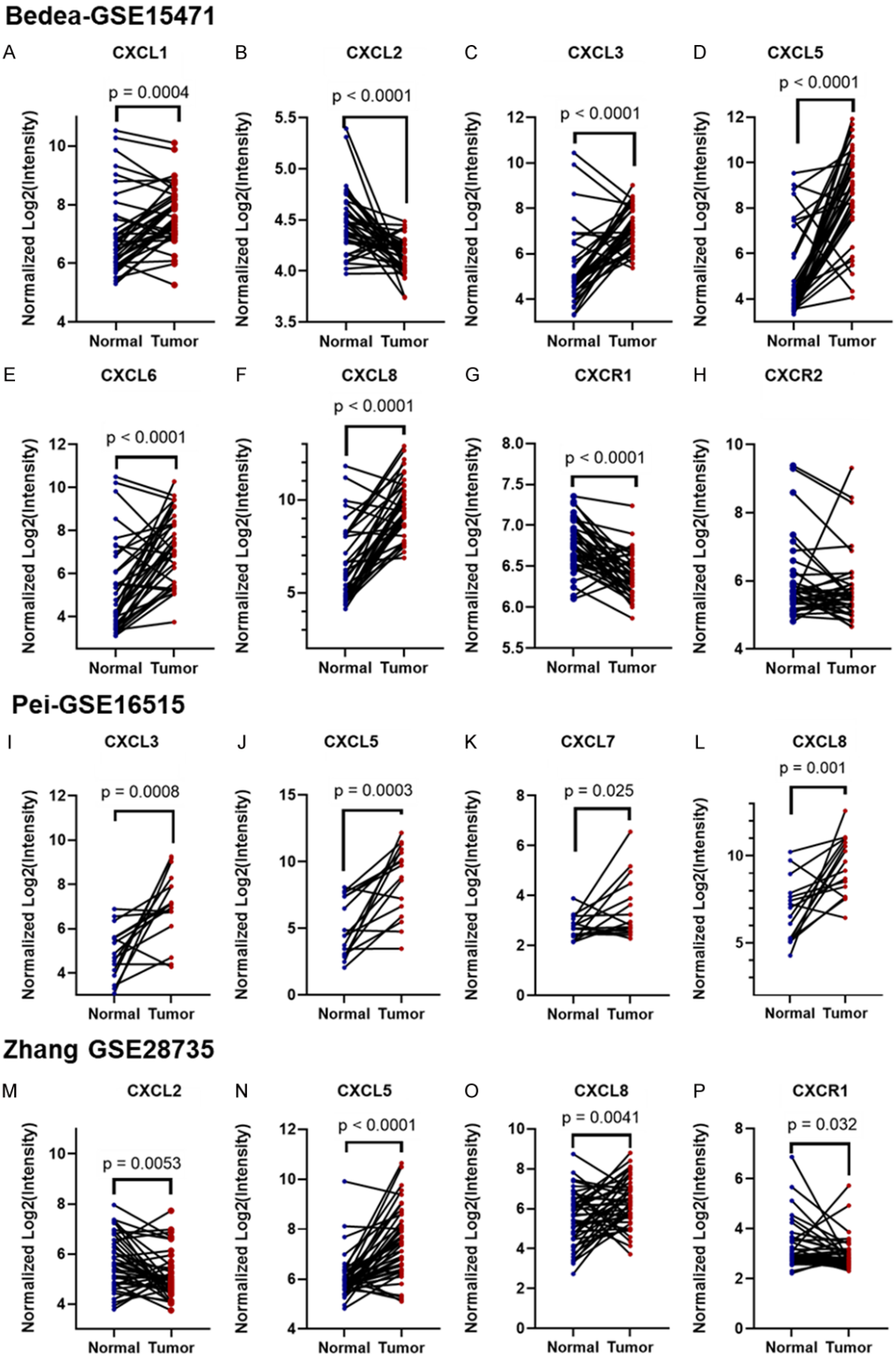
Bedea-GSE15471
A
CXCL1
p = 0.0004
B
CXCL2
p < 0.0001
C
CXCL3
p < 0.0001
D
CXCL5
p < 0.0001
E
CXCL6
p < 0.0001
F
CXCL8
p < 0.0001
G
CXCR1
p < 0.0001
H
CXCR2
Pei-GSE16515
I
CXCL3
p = 0.0008
J
CXCL5
p = 0.0003
K
CXCL7
p = 0.025
L
CXCL8
p = 0.001
Zhang GSE28735
M
CXCL2
p = 0.0053
N
CXCL5
p < 0.0001
O
CXCL8
p = 0.0041
P
CXCR1
p = 0.032
Normalized Log2(Intensity)
Normal Tumor

Figure 2. Analysis of matched normal and tumor in PC patients demonstrate significantly high CXCR2 ligands expression. Analysis of microarray gene expression datasets present in GEO (Badea-GSE15471, Pei-GSE16515, and Zhang-GSE28735) for patients having both matched pancreatic tumors and corresponding normal pancreas samples. (A-H) Graph showing higher trend of CXCL1 (A, P=4E-4), CXCL3 (C, P<1E-4), CXCL5 (D, P<1E-4), CXCL6 (E, P<1E-4), and CXCL8 (F, P<1E-4), lower trend of CXCL2 (B, P<1E-4) and CXCR1 (G, P<1E-4) and non-conclusive trend of CXCR2 expression (H) in Badea dataset with sample size of 34 patients. (I-L) Graph showing significant higher trend of CXCL3 (I, P=8.0E-4), CXCL5 (J, P=3.0E-4), CXCL7 (K, P=2.5E-2) and CXCL8 (L, P=1.0E-3) in Pei dataset with matched sample size of 16 patients. (M-P) Graph showing a significantly higher trend of CXCL2 (M, P=5.3E-3), CXCL5 (N, P<1.0E-4), CXCL8 (O, P=4.1E-3), and CXCR1 (P, P=3.2E-2) in Zhang dataset with a matched sample size of 45 patients.

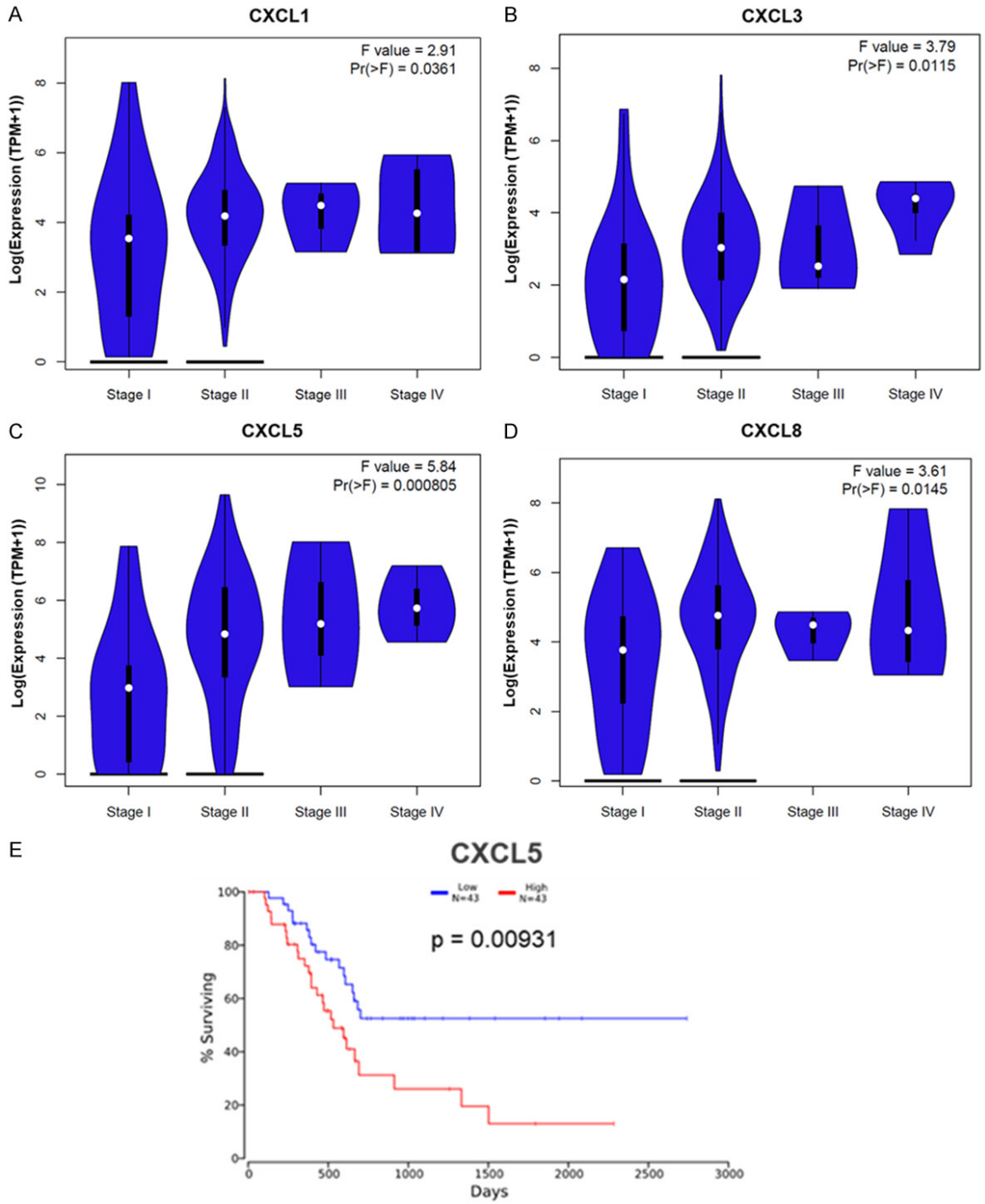

Figure 3. Correlation between CXCR2 ligands expression and different tumor stages of PC patients. (A-D) Violin plots derived from GEPIA online platform demonstrate a comparison of CXCL1 (A), CXCL3 (B), CXCL5 (C), and CXCL8 (D) expression profiles with different tumor stages of PC. CXCL1 [F=2.91, Pr(>F)=0.0361], CXCL3 [F=3.79, Pr(>F)=0.0115], CXCL5 [F=5.84, Pr(>F)=0.000805], and CXCL8 [F=3.61, Pr(>F)=0.0145] were associated and significantly different among the different stages of PC stages. (E) Kaplan-Meier plot showing overall survival analysis of PC patients with low and high CXCL5 expression using online OncoLnc platform. CXCL5 was negatively associated with the overall survival of PC (P=0.00931). Patients with expression above the median are indicated by the red line, and patients with expression below the median are indicated by the blue line.

with lower quartile for survival analysis. PC patients with higher CXCL5 expression demonstrated poor survival. However, this survival analysis is based on various pancreatic samples with different diseases and etiologies such as pancreatic ductal adenocarcinoma, neuroendocrine pancreatic cancer, and others.

CXCL2, CXCL3, and CXCL5 expression in different PC cell lines depends on the cells' aggressive property

We tested the mRNA expression of CXCR2 ligands in eleven different pancreatic cancer cell lines. Three cell lines BxPC-3, Panc-1, and MiaPaCa-2, were derived from primary tumor sites; on the other hand, four cell lines T3M-4, CD18/HPAF, AsPc-1, and Capan-1, were derived from metastatic sites. Also, we used a model of immortalized human pancreatic duct-derived cell lines hTERT-HPNE and hTERT-HPNE-KRAS$^{(G12D)}$. The hTERT-HPNE cell line was developed from the human pancreatic duct by transduction with a retroviral expression vector (pBABEpuro) containing the hTERT gene. Exogenous KRAS$^{(G12D)}$ expression enhances the aggressiveness of the HPNE cells. Also, we utilized a pair of L3.3 and L3.6pl cell lines that differ in their metastatic potential to form liver lesions, with L3.6pl cells being more aggressive than L3.3 cells. For the CXCL1 relative expression profile in these eleven cell lines, we observed a range of expression from 0 to 5000 (**Figure 4A**). The cell lines BxPC-3, Panc-1, and MiaPaCa-2 derived from the primary tumor site showed a lower relative expression of CXCL1 with less than 500. Similar to CXCL2 and CXCL3, cell lines derived from the primary tumor showed CXCL5 expression below 500 and compared HPNE-KRAS to HPNE and L3.6pL to L3.3 that the more aggressive cell lines, HPNE-KRAS and L3.6pL, expressed higher CXCL5. CXCL6 demonstrated a narrow range of relative expression of 0 to 150 with no significant expression trend in cell lines derived from primary or metastatic sites (**Figure 4E**). Most cell lines expressed CXCL1, CXCL5 and CXCL8, and CXCR2 receptor (Supplementary Figure 1). When comparing HPNE-KRAS to HPNE, we observed that HPNE-KRAS showed a higher expression of CXCL1, 3, 5, and 8 (**Figure 4**). In addition, L3.6pL expressed higher expression of CXCL2, 3, and 5 as compared to L3.3. cells (**Figure 4B-D**). In contrast, expression of CXCL6 and 8 was lower in L3.6pl cells as compared to L3.3 cells (**Figure 4E** and **4F**).

CXCL1, CXCL5, and CXCL8 protein expression were lower in BxPC-3, and Panc-1, derived from the primary tumor site (**Figure 5A**) compared to the cell lines derived from metastatic sites. Also, CXCL5 (**Figure 5B**) and CXCL8 (**Figure 5B**) demonstrated higher secretion in HPNE-KRAS aggressive cancer cells than HPNE cells. Interestingly, HPNE cells, pancreatic ductal cells, demonstrated higher expression of CXCL than some metastatic and primary cancer cell lines. We rationalize that each cell line can be considered as a set of individual patient samples. Thus, gene expression levels can vary between normal, and cancer cells in different individuals so do the cell lines. Moreover, online data resources also indicate that certain patients have lower tumor CXCL expression compared to their corresponding normal tissue.

Enhancement of CXCR2 ligands expression in the cancerous lesions of the PC disease progression model

We utilized Pdx1-cre; LSL-Kras$^{(G12D)}$ mice, having a pancreas-specific expression of the KRAS$^{(G12D)}$ mutation [39, 40] as a PC progression model, to understand the precise spatio-temporal pattern for expression of CXCR2 ligands. Pancreatic tissues were derived from the control Pdx1-cre mice (50 weeks) and Pdx1-cre; LSL-Kras$^{(G12D)}$ mice sacrificed at different time points (10, 20, and 50 weeks), including tissues of the liver as a site of metastasis. We observed no expression of CXCR2 (Supplementary Figure 2) and its ligands CXCL1

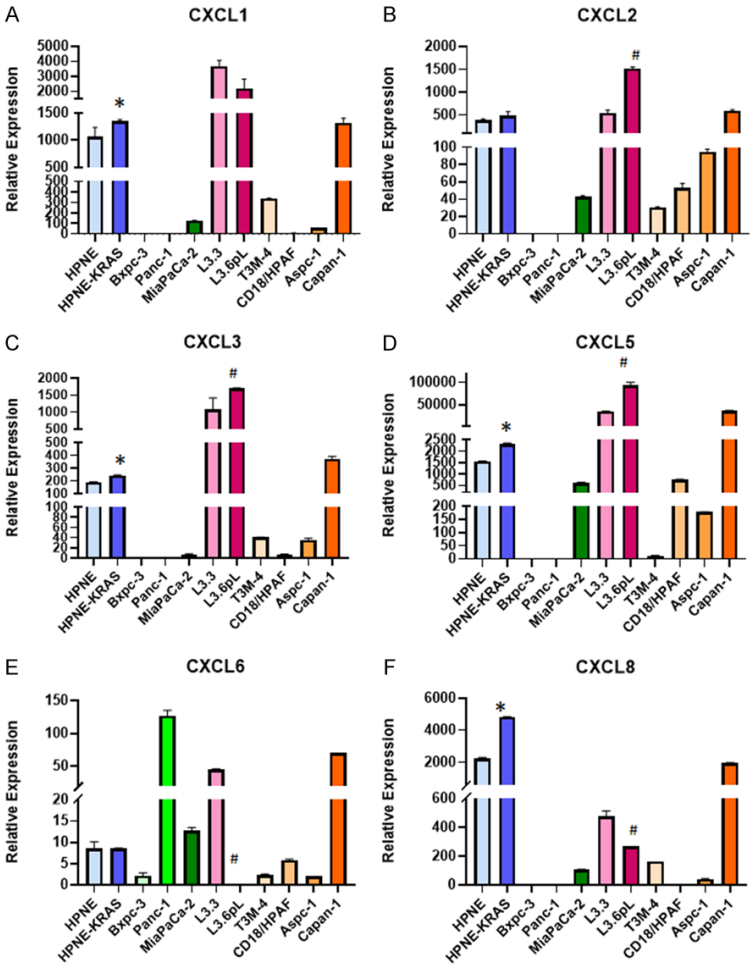

Figure 4. Expression levels of CXCR2 ligands mRNA in different PC cell lines: Bar graph showing relative expression levels of CXCL1 (A), CXCL2 (B), CXCL3 (C), CXCL5 (D), CXCL6 (E), and CXCL8 (F) in the cell lysate of different PC cell lines as determined by quantitative RT-PCR. The values are mean relative expression 2^(-ΔCt) ± standard error of the mean (SEM). *P, 0.05, significantly different from HPNE cells; #P, 0.05, significantly different from L3.3 cells.

(**Figure 6A**), CXCL3 (**Figure 6B**), and CXCL5 (**Figure 6C**) in the pancreas, derived from the control Pdx1-cre mice. However, we observed the expression of CXCR2 and its ligands CXCL1, CXCL3, and CXCL5 in both ductal cells and the surrounding stroma of Pdx1-cre; LSL-Kras$^{(G12D)}$ mice beginning at 10 weeks of age. However, at 10 weeks, the intensity of staining is low, appearing as a background stain. We did not observe any background staining for our antibodies in the negative control sections to rule out the possibility of background staining. The receptor and ligand's expression was further enhanced and became highly specific in the tumors of mice at 20 and 50 weeks of age. Furthermore, liver metastasis derived from Pdx1-cre; LSL-Kras$^{(G12D)}$ mice aged 50 weeks were positive for the expression of CXCR2 as well as the ligands. Thus, our data demonstrate that ductal and stromal cells are a source of CXCR2 expression, along with its ligands, that progressively enhance the developing cancerous lesions of pancreatic tumors and liver metastasis.

High CXCL3 and CXCL8 expression in the pancreatic tumor tissue of the PC patient tissues

Lastly, to confirm our observations in human patient samples, we performed IHC analysis of human CXCL1 (**Figure 7A**), CXCL3 (P<0.05) (**Figure 7B**), and CXCL8 (**Figure 7C**) proteins and CXCR2 (Supplementary Figure 3) receptor in human PC normal and tumor specimens. We detected human CXCL1, CXCL3, and CXCL8 expression in the ducts and the stroma of human PC tumor tissues. Normal pancreatic acinar cells also showed immunoreactivity for human CXCL1; however, the normal pancreatic ducts were negative for its expression (n=3) (**Figure 7A**). Malignant ductal cells (n=14) of PC tissue and surrounding stroma (n=17) showed an enhanced expression of human CXCL1, CXCL3, and CXCL8 compared with the normal pancreas. The average IHC composite score for human CXCL3 (P<0.05) (**Figure 7B**) and CXCL8 (P<0.001) (**Figure 7C**) was significantly higher in pancreatic tumors versus the normal pancreas. In the normal pancreas, the ducts were negative for human CXCL3 and CXCL8; however, the malignant ductal cells showed high immunoreactivity for both the ligands. We observed an intense immunoreactivity for human CXCR2 both in the ducts and the stroma of the human PC specimens (Supplementary Figure 3). CXCR2 was also expressed in the normal pancreas; however,

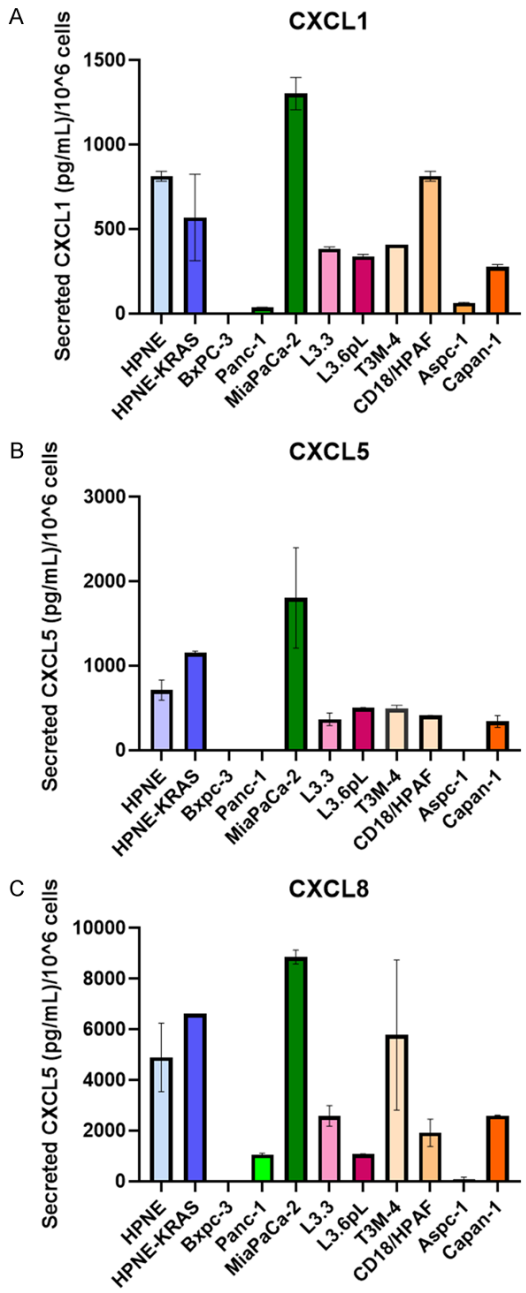

Figure 5. Expression levels of secreted CXCR2 ligands proteins in the supernatant of different PC cell lines: Bar graph showing expression levels of secreted CXCL1 (A), CXCL5 (B), and CXCL8 (C) and in the cell supernatant of different PC cell lines as determined by ELISA. The values are the mean of secretory ligand (pg/mL) per 10^6 cells ± standard deviation (SD).

this expression was localized only to the acinar cell compartment, and normal pancreatic ducts were negative for human CXCR2 expression. Overall, the average composite score of CXCR2 IHC was higher in the PC tissue specimens versus the normal pancreas (P=0.075). We also tested human patients' serum samples for expression of CXCL1, CXCL5, and CXCL8 (P=0.0593) (**Figure 7D**). Of the three tested ligands, only CXCL8 showed a significant difference in expression between normal serum samples and PC patient serum samples.

Discussion

Chemokines are inflammatory mediators with a typical length of 60-90 amino acids and a mass of 8-10 kilodaltons. The prime chemokine function is to recruit leukocytes to an inflammatory area (9). Mainly, chemokines were discovered based on either their biological activity or their expression upon chemical stimulation. The CXC family of chemokines contains 17 members that bind to seven different CXC chemokine receptors (CXCR1-7) [46]. Our current work focuses on the CXC chemokines (CXCL1-3, 5-8) that bind to the CXCR2 receptor.

CXCR2 is a seven-transmembrane G protein-coupled receptor with three extracellular loops necessary for ligand binding and three intracellular loops required for receptor internalization [31]. CXCR2 shares 78% amino acid homology with CXCR1 and binds with all ELR+CXC ligands (CXCL1-3, 5-8); conversely, CXCR1 binds only CXCL6 and CXCL8 [46]. Several cell types, including epithelial cells, endothelial cells, fibroblasts, and immune cells like neutrophils and monocytes, express CXCR2. Hence, cells present in the tumor microenvironment can communicate through CXCR2 and the ligands. Pathologically, there are implications of the CXCR2 biological axis in several autocrine and paracrine tumor-promoting roles in cancer [8, 47], including pancreas [28-30, 48-51], melanoma [24-27], breast [17, 18, 20] and others [14, 23, 52]. However, the normal physiological function of CXCR2 is to regulate neutrophil homeostasis [53] and their recruitment to tumor sites [21, 53, 54]. Additionally, CXCR2 ligands are angiogenic and perform diverse functions. These include facilitating oxygen and nutrient delivery to tumor tissues, attracting and activating human neutrophils, contributing to tumor vascularity, and enhancing tumor invasiveness [8]. Altogether, the CXCLs/CXCR2 axis

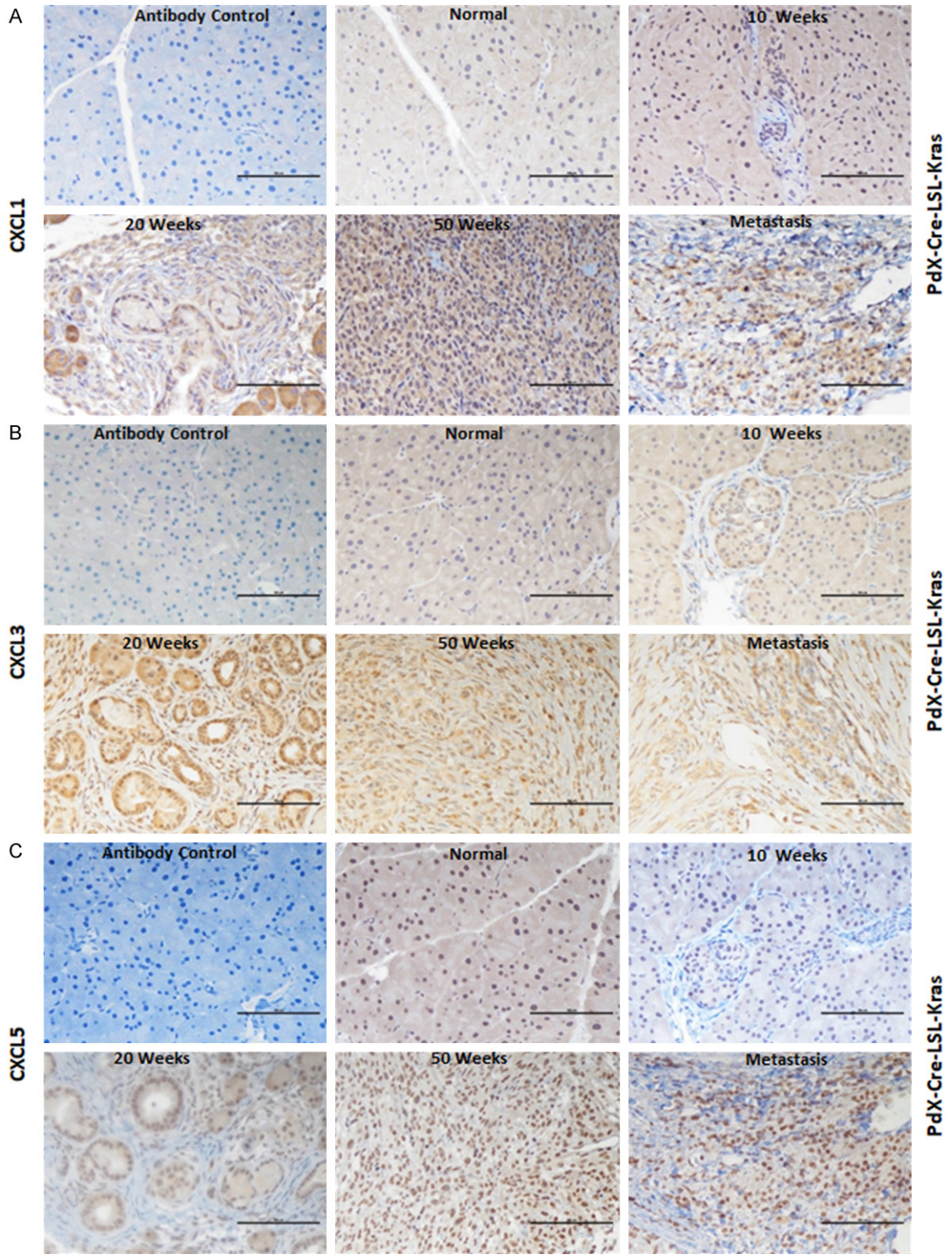

Figure 6. Pathological expression of different CXCR2 ligands in PC progression model derived from tumors and metastasis of Pdx1-cre; LSL-Kras$^{(G12D)}$ (KC) mice: Representative images of CXCL1 (A) CXCL3 (B) and CXCL5 (C) IHC performed on a progression model derived from the normal pancreas (50-weeks), tumors at different ages (10-, 20-, and 50-weeks) and metastasis (liver, 50-weeks) of Pdx1-cre; LSL-Kras$^{(G12D)}$ (KC) mice (n=5). The pictorial graph demonstrates a progressive increase in qualitative CXCL1, CXCL3, and CXCL5 expression in cancerous lesions of the KC mice model until 50-weeks with positive expression of these ligands in liver metastasis of 50-weeks mice. The normal pancreas of 50-week old Pdx1-cre mice was negative for CXCL1, CXCL3, and CXCL5 expression. The scale bar represents 100 μm.

A

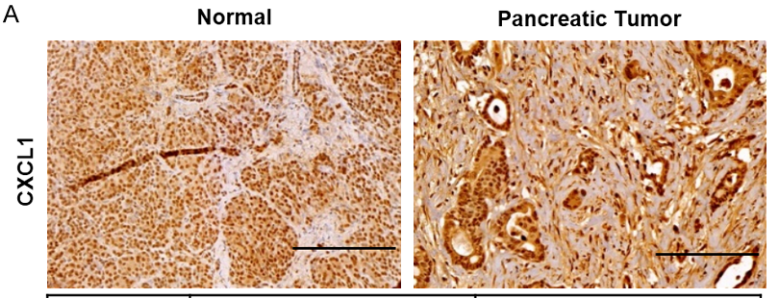

	Normal Pancreas		Primary Tumor	
	Ducts	Other cells	Ducts	Stroma
CXCL1 +VE	0/3 (0%)	3/3 (100%)	14/14 (100%)	16/16 (100%)
CXCL1 -VE	3/3 (100%)	0/3 (0%)	0/14 (0%)	0/16 (0%)

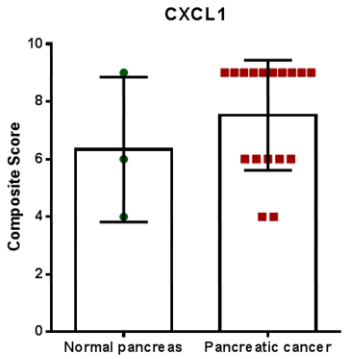

B

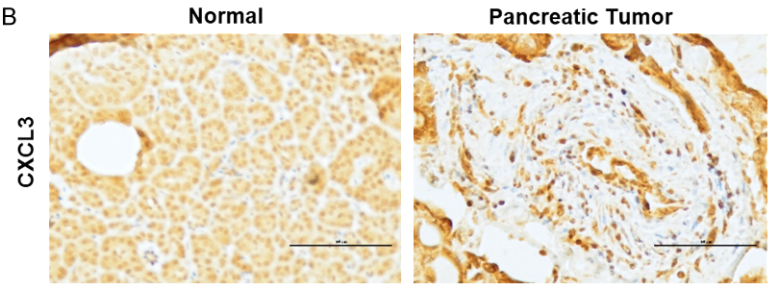

	Normal Pancreas		Primary Tumor	
	Ducts	Other cells	Ducts	Stroma
CXCL3 +VE	0/3 (0%)	3/3 (100%)	12/12 (100%)	17/17 (100%)
CXCL3 -VE	3/3 (100%)	0/3 (0%)	0/12 (0%)	0/17 (0%)

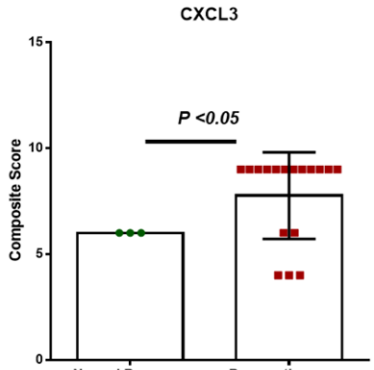

C

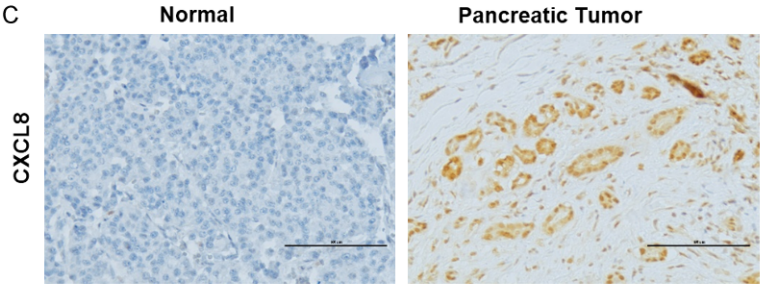

	Normal Pancreas		Primary tumor	
	Ducts	Other cells	Ducts	Stroma
CXCL8 +VE	0/3 (0%)	3/3 (100%)	12/12 (100%)	17/17 (100%)
CXCL8 -VE	3/3 (100%)	0/3 (0%)	0/12 (0%)	0/17 (0%)

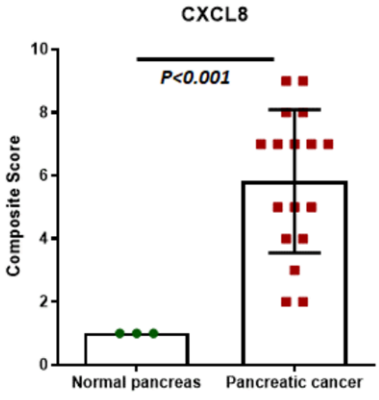

D

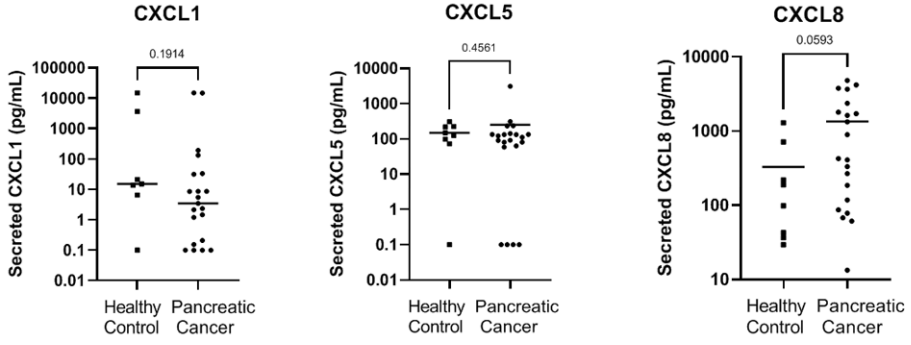

Figure 7. Pathological expression of different CXCR2 ligands in PC patients: Representative images of CXCL1 (A), CXCL3 (B), and CXCL8 (C) IHC performed on the normal human pancreas and tumor tissue cores present in the TMA. Bar graph demonstrates quantitation of IHC score of CXCL1 (A), CXCL3 (B), and CXCL8 staining in pancreatic tumor tissues. The scale bar represents 100 μm. The bar graph shows higher CXCL3 ($P<0.05$) and CXCL8 ($P<0.01$) IHC scores in the tumor in comparison with a normal pancreas. (D) Graph showing levels of secreted CXCL1, CXCL5, and CXCL8 in serum samples of PC patients. Secreted CXCL8 is significantly higher in serum of PC patients in comparison with healthy controls (0.0593).

regulates tumor angiogenesis, metastasis, and even chemoresistance in different cancers.

Apart from the pathological functions mentioned above, upregulation of the ligands for CXCR2 is a well-known consequence of activating mutations in the KRAS oncogene [29]. Matsuo et al. identified the link between $KRAS^{(G12V)}$ and $KRAS^{(G12D)}$ mutations and upregulation of cumulative expression of CXCL1, CXCL5, and CXCL8 in PC. Later, Hayer et al. reported that knock-down of endogenous $KRAS^{(G12D)}$ in the PC cell line SW1990 reduced transcripts of CXCL1-3, 5-8. Based on the link that 90% of PC patients have the oncogenic KRAS mutation that can upregulate the ligands for CXCR2, we explored the potential of CXCR2 ligands as a biomarker in this study in PC.

We utilized different online portals such as Oncomine, MiPanda, and Gepia to strengthen our examination of the expression pattern of CXCR2 ligands in normal pancreas and pancreatic tumors. Analysis from different online portals demonstrated that expression of all CXCR2 ligands except CXCL2 and CXCL7 were significantly upregulated in one of three online portals. CXCR2 expression, on the other hand, did not show any significant difference, whereas homologous CXCR1 was significantly decreased in pancreatic tumors compared to normal pancreas. We would expect that upregulation of the ligands usually leads to downregulation of expression of their corresponding receptor. Next, we compared CXCR2 ligands expression between matched normal and adjacent tumors of the pancreas to examine whether our observations hold valid samples from the same individual. This approach also offers better visualization of trends and differences in the range of CXCR2 ligand expression in tumor and normal tissue of an individual. Towards this end, we utilized matched microarray gene expression profile-from GSE15471, GSE16515, and GSE28735 datasets from the GEO database and observed similar results as those obtained from the online portals. We also visualized the distribution of different CXCR2 ligand expressions in pathological stages of PC and observed that only CXCL1, CXCL3, CXCL5, and CXCL8 were significantly related to stages of PC. Also, among seven ligands of CXCR2, only CXCL5 demonstrated a significant correlation with the survival of PC patients. Although CXCL1, CXCL3, CXCL6, and CXCL8 demonstrated the characteristics of potential biomarkers, CXCL5 can be regarded as the most promising candidate. Apart from significant correlation with the survival of PC patients, CXCL5 was also the most upregulated CXC ligand in the PC patients with a non-overlapping interquartile range of CXCL5 expression in normal and PC tumor and distinct pattern of increasing expression and narrowing range with the later pathological PC stages.

We validated CXCR2 ligand expression analysis obtained through the data mining platforms by performing different experimental approaches. Firstly, we examined the CXCR2 ligand expression using a panel of PC cell lines. We categorized these cell lines based on their derivation from primary tumor sites, metastatic sites, aggressiveness, and metastatic potential. We observed that the expression of CXCL2, CXCL3, and CXCL5 was higher in cell lines derived from metastatic sites and with high aggressiveness and metastatic ability. Next, we utilized disease progression PDX-cre-LSL-$KRAS^{(G12D)}$ mouse model of PC and human PC tissue specimens to identify the cellular sources of the expression of CXCR2 ligands. We were using pancreatic tissues derived from the PDX-cre-LSL-$KRAS^{(G12D)}$ mouse model; we wanted to recognize the expression pattern of CXCR2 and its ligand during the development and progression of PC. The PDX-cre-LSL-$KRAS^{(G12D)}$ mouse model, having pancreas-specific knock-in for the $KRAS^{(G12D)}$ mutation, is known to closely recapitulate the histological and molecular pathology of the human PC [55]. This model enables the evaluation of the cellular pattern for the expression of desired molecular targets and helps identify their time points during disease development.

Moreover, PC is associated with a high frequency of mutations in the KRAS oncogene in the malignant ductal cells and dense stroma production. CXCR2 and its ligands are known to be expressed by several cell types in the body, including part of the PC tumor microenvironment, such as fibroblasts, immune cells, and endothelial cells. Thus, precise identification of the cell types expressing CXCR2 and its ligands in PC can lead to target specificity. We identified the expression of mouse CXCL1, CXCL3, and CXCL5 and mouse CXCR2 in the pre-cancerous lesions of PDX-cre-LSL-Kras$^{(G12D)}$ mice. The normal murine pancreas was negative for the expression of mouse CXCR2, CXCL1, and CXCL5. The expression of the ligands and the receptor intensified with the progression of the disease.

Next, we evaluated the expression pattern of CXCL1 and CXCL3, and CXCL8 in the human PC tissue specimens. Previous reports have already elaborately demonstrated the expression of CXCL5 in human PC patient tumor specimens, discussed later. Our results show CXCL1, CXCL3, CXCL8, and CXCR2 expression in the human pancreatic tumors and the normal pancreas. We identified CXCL1, CXCL3, and CXCL8 in malignant ductal cells and surrounding stroma of the PC tissues. Also, we observed positive immunoreactivity for CXCR2 only in the acinar cells of the normal pancreas; however, both malignant ducts and stroma were positive in the tumor tissues. Moreover, the expression of CXCL3 and CXCL8 was higher in the pancreatic tumors than in the normal pancreas. Like our observations, human CXCR2 has been reported in both PC tissues and the normal pancreas [50, 56, 57]. Similarly, a previous report by Frick et al. demonstrated a non-significant increase in the expression of human CXCL1 in the PC tissues versus the surrounding normal pancreas [58].

Lastly, we evaluated CXCL1, CXCL5, and CXCL8 in the serum of eight healthy controls and twenty PC patients. We observed that only CXCL8 is significantly higher in PC patients in comparison with the healthy controls. The lack of significant difference in CXCL1 and CXCL5 serum levels could be because of the small sample size of the patients. Previously, reports have evaluated the expression of different CXC chemokines in human PC tissues and serum samples. O'Hayer et al. evaluated the expression of CXCL1, CXCL5, CXCL6, CXCL7, and CXCL8 in serum samples isolated from 20 PC patients and 19 age- and sex-matched healthy donors. Their results demonstrated significantly elevated expression of CXCL1 and CXCL7 in PC specimens. No change in the expression of CXCL5, CXCL6, and CXCL8 was observed in PC serum specimens compared with healthy donors [59]. Moreover, a recent study reported significantly higher levels of CXCL8 in serum samples of PC patients compared with specimens derived from patients of acute or chronic pancreatitis [60]. Matsuo et al. evaluated CXCL1, CXCL5, and CXCL8 in the secretin stimulated pancreatic exocrine secretions of PC patients and normal individuals. Their data demonstrate significantly enhanced secretion of CXCL5 in PC patients versus normal individuals. However, they did not observe a significant change in the individual expression of CXCL1 and CXCL8 [61].

Apart from our transcriptome analysis using different available online tools and experimental results that suggest the relevance of CXCL5 as a biomarker, various recent research reports provide extensive evidence for the expression and pathological role of CXCL5 in PC [14, 62-64]. CXCL5 is a potential biomarker in different cancers [14, 59-65] and is also included in the eight gene molecular signatures for PC prognosis [65]. Significantly increased CXCL5 was reported in the tumor tissue lysates of PC compared with the normal tissue and histopathologically distinct diseases of the pancreas. Furthermore, CXCL5 was shown to localize in the cytoplasm of the malignant ductal cells. In contrast, the surrounding normal tissues demonstrated no expression for the ligand except in some acinar cells and islets of Langerhans [66]. Later Li et al. identified that the expression of CXCL5 was occasionally present in PanIN-1 lesions but increased in PanIN-2 and PanIN-3 stages, where 4 out of the total 11 specimens demonstrated high immunoreactivity for CXCL5 [67]. Moreover, CXCL5 was detected in 67% of PC specimens with staining of apical cytoplasm in the tumor cells and no immunoreactivity in the acinar and ductal epithelium of the normal pancreas. Furthermore, they established that high CXCL5 expression correlates with tumor progression and shortened patient survival time by performing Kaplan-Meier analysis. Lastly, the authors report-

ed that higher microvessel density in the tumor correlates with higher expression of CXCL5, suggesting its role in neoangiogenesis [67]. Recent reports by Wu et al. demonstrate similar results as discussed above. They suggest that high CXCL5 expression is positively correlated with poor survival [68] and the increased infiltration of immune suppressive cells [69]. Unfortunately, we did not observe a significant difference in CXCL5 expression in serum samples between healthy controls and PC patients, limiting its utility as a biomarker. However, we must consider that our observations are based on a limited number of PC patient serum samples. Overall, there is a need to test CXCL5 expression in a larger cohort of PC patients.

Compared with other members of its family, CXCL8 is the most extensively studied ligand for its pathological significance in PC [49, 52] and evaluated for the potential of biomarkers [70-72]. The first report of higher expression of CXCL8 protein in human PC tissue specimens (n=45) compared with the normal pancreas (n=15) was by Xiangdong et al. (2000). Its expression was localized to the ductal cells as well as the stroma [73]. Later, Kuwada et al. (2002) reported the expression of CXCL8, primarily in the cytoplasm of the tumor cells, in 20 out of 50 patient tissue specimens evaluated [74]. Another group identified higher expression of CXCL8 protein in PC tumor lysates compared to non-affected neighboring tissue. The group also demonstrated that the expression of CXCL8 was upregulated in the T3 and T4 versus the T1 and T2 stages of PC based on the TNM classification of malignant tumors. Furthermore, their IHC analysis revealed that CXCL8 was in the cytoplasm of the ductal epithelial cells and the infiltrating inflammatory cells CXCL8 [66]. In contrast to this report that did not detect CXCL8 in the normal pancreas, a recent study detected expression of CXCL8 in both PC (55.6%) and non-cancer tissues (25.9%) [60].

Introduction of novel biomarkers are critically needed to improve the management of patients with pancreatic cancer [75]. Currently, serum carbohydrate antigen 19-9 (CA19-9) is utilized in the diagnostic work-up of patients diagnosed with PC however this biomarker lacks the sensitivity and specificity associated with a gold-standard marker. Recent reports have evaluated the clinical usefulness of CXCR2 and its ligands in diagnosis and prediction of PC compared to classic biomarkers [70, 76]. The diagnostic sensitivity, accuracy, negative predictive value, and areas under the receiver operating characteristic curves for serum CXCL8 were higher than those for serum CXCR2, C-reactive protein, CA 19-9, and carcinoembryonic antigen. Moreover, serum CXCL8 and CXCR2 were the only significant predictor of PC risk [70, 76]. Together these studies suggest that tumor tissue expression and serum levels of CXCR2 and its ligands will be clinically potential biomarkers alone or in combination with classic ones. Besides, the expression of CXCR2 chemokines is associated with survival analysis of different cancer patients, suggesting the potential of these ligands as a prognostic marker in the future. CXCR2 ligand expression can also find utility as “molecular signatures” to determine tumor aggressiveness, pathological stages, selection of appropriate treatments, and response to chemotherapy drugs for cancer patients.

However, taking advantage of CXCR2 ligands for diagnostic and prognostic biomarkers can be challenging for various reasons (14). Firstly, both tumor cells and a wide range of host cells can express CXCR2 ligands. The expression of these ligands is not limited to PC but also other cancers and chronic inflammatory diseases such as rheumatoid arthritis and AIDS. Secondly, some CXCR2 ligands demonstrate promiscuous nature by binding to CXCR1, which increases their interaction’s complexity, and may show compensatory effects under different pathological conditions. Thirdly, CXCR2 ligands profile changes with PC cancer stages, drug treatment, and chemotherapy resistance, again complicating the specificity of biomarker usage. In conclusion, the current understanding of CXCR2 ligands suggests combining multiple pairs of CXCR2 ligands or using them with other biomarker molecules for diagnostic and prognostic purposes.

Acknowledgements

This work was supported in part by grants R01CA228524; Cancer Center Support Grant (P30CA036727); SPORE in Pancreatic Cancer, P50CA127297; Pancreatic Cancer Detection Consortium, U01CA210240; and NCI Research Specialist, R50CA211462 from the National Cancer Institute, National Institutes of Health.

The serum samples were obtained under the Institutional Review Boards (IRB) of the University of Nebraska Medical Center (UNMC) (IRB number 209-00). Consent was obtained from all patients and controls before enrollment into the study. Inclusion criteria were any adult patient (age ≥18 years) with histologically proven PC. Chronic pancreatitis (CP) was defined based on CT scan findings of calcifications, abnormal pancreatogram or secretin stimulation test.

Disclosure of conflict of interest

None.

Address correspondence to: Dr. Rakesh K Singh, Department of Pathology and Microbiology, 985-950 Nebraska Medical Center, Omaha, NE 68198-5900, USA. Tel: 402-559-9949; Fax: 402-559-5900; E-mail: rsingh@unmc.edu

References

[1] Zhang L, Sanagapalli S and Stoita A. Challenges in diagnosis of pancreatic cancer. World J Gastroenterol 2018; 24: 2047-2060.

[2] Ho WJ, Jaffee EM and Zheng L. The tumour microenvironment in pancreatic cancer - clinical challenges and opportunities. Nat Rev Clin Oncol 2020; 17: 527-540.

[3] Singhi AD, Koay EJ, Chari ST and Maitra A. Early detection of pancreatic cancer: opportunities and challenges. Gastroenterology 2019; 156: 2024-2040.

[4] Lowenfels AB and Maisonneuve P. Epidemiology and risk factors for pancreatic cancer. Best Pract Res Clin Gastroenterol 2006; 20: 197-209.

[5] Legler DF, Loetscher M, Roos RS, Clark-Lewis I, Baggiolini M and Moser B. B cell-attracting chemokine 1, a human CXC chemokine expressed in lymphoid tissues, selectively attracts B lymphocytes via BLR1/CXCR5. J Exp Med 1998; 187: 655-660.

[6] Zlotnik A and Yoshie O. Chemokines: a new classification system and their role in immunity. Immunity 2000; 12: 121-127.

[7] Baggiolini M, Dewald B and Moser B. Interleukin-8 and related chemotactic cytokines--CXC and CC chemokines. Adv Immunol 1994; 55: 97-179.

[8] Saxena S and Singh RK. Chemokines orchestrate tumor cells and the microenvironment to achieve metastatic heterogeneity. Cancer Metastasis Rev 2021; 40: 447-476.

[9] Baggiolini M, Dewald B and Moser B. Human chemokines: an update. Annu Rev Immunol 1997; 15: 675-705.

[10] Strieter RM, Polverini PJ, Kunkel SL, Arenberg DA, Burdick MD, Kasper J, Dzuiba J, Van Damme J, Walz A, Marriott D, et al. The functional role of the ELR motif in CXC chemokine-mediated angiogenesis. J Biol Chem 1995; 270: 27348-27357.

[11] Scapini P, Morini M, Tecchio C, Minghelli S, Di Carlo E, Tanghetti E, Albini A, Lowell C, Berton G, Noonan DM and Cassatella MA. CXCL1/macrophage inflammatory protein-2-induced angiogenesis in vivo is mediated by neutrophil-derived vascular endothelial growth factor-A. J Immunol 2004; 172: 5034-5040.

[12] Belperio JA, Keane MP, Arenberg DA, Addison CL, Ehlert JE, Burdick MD and Strieter RM. CXC chemokines in angiogenesis. J Leukoc Biol 2000; 68: 1-8.

[13] Strieter RM, Kunkel SL, Arenberg DA, Burdick MD and Polverini PJ. Interferon gamma-inducible protein 10 (IP-10), a member of the C-X-C chemokine family, is an inhibitor of angiogenesis. Biochem Biophys Res Commun 1995; 210: 51-57.

[14] Saintigny P, Massarelli E, Lin S, Ahn YH, Chen Y, Goswami S, Erez B, O'Reilly MS, Liu D, Lee JJ, Zhang L, Ping Y, Behrens C, Solis Soto LM, Heymach JV, Kim ES, Herbst RS, Lippman SM, Wistuba II, Hong WK, Kurie JM and Koo JS. CXCR2 expression in tumor cells is a poor prognostic factor and promotes invasion and metastasis in lung adenocarcinoma. Cancer Res 2013; 73: 571-582.

[15] Gold KA, Kim ES, Liu DD, Yuan P, Behrens C, Solis LM, Kadara H, Rice DC, Wistuba II, Swisher SG, Hofstetter WL, Lee JJ and Hong WK. Prediction of survival in resected non-small cell lung cancer using a protein expression-based risk model: implications for personalized chemoprevention and therapy. Clin Cancer Res 2014; 20: 1946-1954.

[16] Nannuru KC, Sharma B, Varney ML and Singh RK. Role of chemokine receptor CXCR2 expression in mammary tumor growth, angiogenesis and metastasis. J Carcinog 2011; 10: 40.

[17] Sharma B, Nannuru KC, Saxena S, Varney ML and Singh RK. CXCR2: a novel mediator of mammary tumor bone metastasis. Int J Mol Sci 2019; 20: 1237.

[18] Sharma B, Nannuru KC, Varney ML and Singh RK. Host Cxcr2-dependent regulation of mammary tumor growth and metastasis. Clin Exp Metastasis 2015; 32: 65-72.

[19] Sharma B, Nawandar DM, Nannuru KC, Varney ML and Singh RK. Targeting CXCR2 enhances chemotherapeutic response, inhibits mammary tumor growth, angiogenesis, and lung metastasis. Mol Cancer Ther 2013; 12: 799-808.

[20] Sharma B, Varney ML, Saxena S, Wu L and Singh RK. Induction of CXCR2 ligands, stem cell-like phenotype, and metastasis in chemo-

therapy-resistant breast cancer cells. Cancer Lett 2016; 372: 192-200.
[21] Wu L, Awaji M, Saxena S, Varney ML, Sharma B and Singh RK. IL-17-CXC chemokine receptor 2 axis facilitates breast cancer progression by up-regulating neutrophil recruitment. Am J Pathol 2020; 190: 222-233.
[22] An H, Xu L, Chang Y, Zhu Y, Yang Y, Chen L, Lin Z and Xu J. CXC chemokine receptor 2 is associated with postoperative recurrence and survival of patients with non-metastatic clear-cell renal cell carcinoma. Eur J Cancer 2015; 51: 1953-1961.
[23] Li L, Xu L, Yan J, Zhen ZJ, Ji Y, Liu CQ, Lau WY, Zheng L and Xu J. CXCR2-CXCL1 axis is correlated with neutrophil infiltration and predicts a poor prognosis in hepatocellular carcinoma. J Exp Clin Cancer Res 2015; 34: 129.
[24] Singh RK and Varney ML. Regulation of interleukin 8 expression in human malignant melanoma cells. Cancer Res 1998; 58: 1532-1537.
[25] Singh S, Singh AP, Sharma B, Owen LB and Singh RK. CXCL8 and its cognate receptors in melanoma progression and metastasis. Future Oncol 2010; 6: 111-116.
[26] Singh S, Varney M and Singh RK. Host CXCR2-dependent regulation of melanoma growth, angiogenesis, and experimental lung metastasis. Cancer Res 2009; 69: 411-415.
[27] Wu S, Saxena S, Varney ML and Singh RK. CXCR1/2 chemokine network regulates melanoma resistance to chemotherapies mediated by NF-κB. Curr Mol Med 2017; 17: 436-449.
[28] Awaji M, Saxena S, Wu L, Prajapati DR, Purohit A, Varney ML, Kumar S, Rachagani S, Ly QP, Jain M, Batra SK and Singh RK. CXCR2 signaling promotes secretory cancer-associated fibroblasts in pancreatic ductal adenocarcinoma. FASEB J 2020; 34: 9405-9418.
[29] Purohit A, Varney M, Rachagani S, Ouellette MM, Batra SK and Singh RK. CXCR2 signaling regulates KRAS($G^{12}D$)-induced autocrine growth of pancreatic cancer. Oncotarget 2016; 7: 7280-7296.
[30] Purohit A, Saxena S, Varney M, Prajapati DR, Kozel JA, Lazenby A and Singh RK. Host Cxcr2-dependent regulation of pancreatic cancer growth, angiogenesis, and metastasis. Am J Pathol 2021; 191: 759-771.
[31] Hertzer KM, Donald GW and Hines OJ. CXCR2: a target for pancreatic cancer treatment? Expert Opin Ther Targets 2013; 17: 667-680.
[32] Steele CW, Karim SA, Leach JDG, Bailey P, Upstill-Goddard R, Rishi L, Foth M, Bryson S, McDaid K, Wilson Z, Eberlein C, Candido JB, Clarke M, Nixon C, Connelly J, Jamieson N, Carter CR, Balkwill F, Chang DK, Evans TRJ, Strathdee D, Biankin AV, Nibbs RJB, Barry ST, Sansom OJ and Morton JP. CXCR2 inhibition profoundly suppresses metastases and augments immunotherapy in pancreatic ductal adenocarcinoma. Cancer Cell 2016; 29: 832-845.
[33] Badea L, Herlea V, Dima SO, Dumitrascu T and Popescu I. Combined gene expression analysis of whole-tissue and microdissected pancreatic ductal adenocarcinoma identifies genes specifically overexpressed in tumor epithelia. Hepatogastroenterology 2008; 55: 2016-2027.
[34] Pei H, Li L, Fridley BL, Jenkins GD, Kalari KR, Lingle W, Petersen G, Lou Z and Wang L. FKBP51 affects cancer cell response to chemotherapy by negatively regulating Akt. Cancer Cell 2009; 16: 259-266.
[35] Zhang G, Schetter A, He P, Funamizu N, Gaedcke J, Ghadimi BM, Ried T, Hassan R, Yfantis HG, Lee DH, Lacy C, Maitra A, Hanna N, Alexander HR and Hussain SP. DPEP1 inhibits tumor cell invasiveness, enhances chemosensitivity and predicts clinical outcome in pancreatic ductal adenocarcinoma. PLoS One 2012; 7: e31507.
[36] Rhodes DR, Yu J, Shanker K, Deshpande N, Varambally R, Ghosh D, Barrette T, Pandey A and Chinnaiyan AM. ONCOMINE: a cancer microarray database and integrated data-mining platform. Neoplasia 2004; 6: 1-6.
[37] Tang Z, Li C, Kang B, Gao G, Li C and Zhang Z. GEPIA: a web server for cancer and normal gene expression profiling and interactive analyses. Nucleic Acids Res 2017; 45: W98-W102.
[38] Niknafs YS, Pandian B, Gajjar T, Gaudette Z, Wheelock K, Maz MP, Achar RK, Song M, Massaro C, Cao X and Chinnaiyan AM. Mipanda: a resource for analyzing and visualizing next-generation sequencing transcriptomics data. Neoplasia 2018; 20: 1144-1149.
[39] Anaya J. OncoLnc: linking TCGA survival data to mRNAs, miRNAs, and lncRNAs. PeerJ Comput Sci 2016; 2: e67.
[40] Bruns CJ, Harbison MT, Kuniyasu H, Eue I and Fidler IJ. In vivo selection and characterization of metastatic variants from human pancreatic adenocarcinoma by using orthotopic implantation in nude mice. Neoplasia 1999; 1: 50-62.
[41] Campbell PM, Groehler AL, Lee KM, Ouellette MM, Khazak V and Der CJ. K-Ras promotes growth transformation and invasion of immortalized human pancreatic cells by Raf and phosphatidylinositol 3-kinase signaling. Cancer Res 2007; 67: 2098-2106.
[42] Saxena S, Hayashi Y, Wu L, Awaji M, Atri P, Varney ML, Purohit A, Rachagani S, Batra SK and Singh RK. Pathological and functional significance of Semaphorin-5A in pancreatic cancer progression and metastasis. Oncotarget 2018; 9: 5931-5943.

[43] Saxena S, Purohit A, Varney ML, Hayashi Y and Singh RK. Semaphorin-5A maintains epithelial phenotype of malignant pancreatic cancer cells. BMC Cancer 2018; 18: 1283.
[44] Wu L, Saxena S, Goel P, Prajapati DR, Wang C and Singh RK. Breast cancer cell-neutrophil interactions enhance neutrophil survival and pro-tumorigenic activities. Cancers (Basel) 2020; 12: 2884.
[45] Hingorani SR, Petricoin EF, Maitra A, Rajapakse V, King C, Jacobetz MA, Ross S, Conrads TP, Veenstra TD, Hitt BA, Kawaguchi Y, Johann D, Liotta LA, Crawford HC, Putt ME, Jacks T, Wright CV, Hruban RH, Lowy AM and Tuveson DA. Preinvasive and invasive ductal pancreatic cancer and its early detection in the mouse. Cancer Cell 2003; 4: 437-450.
[46] Lazennec G and Richmond A. Chemokines and chemokine receptors: new insights into cancer-related inflammation. Trends Mol Med 2010; 16: 133-144.
[47] Cheng Y, Ma XL, Wei YQ and Wei XW. Potential roles and targeted therapy of the CXCLs/CXCR2 axis in cancer and inflammatory diseases. Biochim Biophys Acta Rev Cancer 2019; 1871: 289-312.
[48] Matsuo Y, Campbell PM, Brekken RA, Sung B, Ouellette MM, Fleming JB, Aggarwal BB, Der CJ and Guha S. K-Ras promotes angiogenesis mediated by immortalized human pancreatic epithelial cells through mitogen-activated protein kinase signaling pathways. Mol Cancer Res 2009; 7: 799-808.
[49] Matsuo Y, Ochi N, Sawai H, Yasuda A, Takahashi H, Funahashi H, Takeyama H, Tong Z and Guha S. CXCL8/IL-8 and CXCL12/SDF-1alpha co-operatively promote invasiveness and angiogenesis in pancreatic cancer. Int J Cancer 2009; 124: 853-861.
[50] Matsuo Y, Raimondo M, Woodward TA, Wallace MB, Gill KR, Tong Z, Burdick MD, Yang Z, Strieter RM, Hoffman RM and Guha S. CXC-chemokine/CXCR2 biological axis promotes angiogenesis in vitro and in vivo in pancreatic cancer. Int J Cancer 2009; 125: 1027-1037.
[51] Matsuo Y, Takeyama H and Guha S. Cytokine network: new targeted therapy for pancreatic cancer. Curr Pharm Des 2012; 18: 2416-2419.
[52] Liu Q, Li A, Tian Y, Wu JD, Liu Y, Li T, Chen Y, Han X and Wu K. The CXCL8-CXCR1/2 pathways in cancer. Cytokine Growth Factor Rev 2016; 31: 61-71.
[53] Wu L, Saxena S, Awaji M and Singh RK. Tumor-associated neutrophils in cancer: going pro. Cancers (Basel) 2019; 11: 564.
[54] Mei J, Liu Y, Dai N, Hoffmann C, Hudock KM, Zhang P, Guttentag SH, Kolls JK, Oliver PM, Bushman FD and Worthen GS. Cxcr2 and Cxcl5 regulate the IL-17/G-CSF axis and neutrophil homeostasis in mice. J Clin Invest 2012; 122: 974-986.
[55] Hingorani SR, Wang L, Multani AS, Combs C, Deramaudt TB, Hruban RH, Rustgi AK, Chang S and Tuveson DA. Trp53R172H and KrasG12D cooperate to promote chromosomal instability and widely metastatic pancreatic ductal adenocarcinoma in mice. Cancer Cell 2005; 7: 469-483.
[56] Sun X, He X, Zhang Y, Hosaka K, Andersson P, Wu J, Wu J, Jing X, Du Q, Hui X, Ding B, Guo Z, Hong A, Liu X, Wang Y, Ji Q, Beyaert R, Yang Y, Li Q and Cao Y. Inflammatory cell-derived CXCL3 promotes pancreatic cancer metastasis through a novel myofibroblast-hijacked cancer escape mechanism. Gut 2022; 71: 129-147.
[57] Litman-Zawadzka A, Łukaszewicz-Zając M, Gryko M, Kulczyńska-Przybik A, Kędra B and Mroczko B. Specific receptors for the chemokines CXCR2 and CXCR4 in pancreatic cancer. Int J Mol Sci 2020; 21: 6193.
[58] Frick VO, Rubie C, Wagner M, Graeber S, Grimm H, Kopp B, Rau BM and Schilling MK. Enhanced ENA-78 and IL-8 expression in patients with malignant pancreatic diseases. Pancreatology 2008; 8: 488-497.
[59] O'Hayer KM, Brady DC and Counter CM. ELR+ CXC chemokines and oncogenic Ras-mediated tumorigenesis. Carcinogenesis 2009; 30: 1841-1847.
[60] Chen Y, Shi M, Yu GZ, Qin XR, Jin G, Chen P and Zhu MH. Interleukin-8, a promising predictor for prognosis of pancreatic cancer. World J Gastroenterol 2012; 18: 1123-9.
[61] Huang J, Chen Z, Ding C, Lin S, Wan D and Ren K. Prognostic biomarkers and immunotherapeutic targets among CXC chemokines in pancreatic adenocarcinoma. Front Oncol 2021; 11: 711402.
[62] Ando Y, Ohuchida K, Otsubo Y, Kibe S, Takesue S, Abe T, Iwamoto C, Shindo K, Moriyama T, Nakata K, Miyasaka Y, Ohtsuka T, Oda Y and Nakamura M. Necroptosis in pancreatic cancer promotes cancer cell migration and invasion by release of CXCL5. PLoS One 2020; 15: e0228015.
[63] Chao T, Furth EE and Vonderheide RH. CXCR2-dependent accumulation of tumor-associated neutrophils regulates T-cell immunity in pancreatic ductal adenocarcinoma. Cancer Immunol Res 2016; 4: 968-982.
[64] Zhang W, Wang H, Sun M, Deng X, Wu X, Ma Y, Li M, Shuoa SM, You Q and Miao L. CXCL5/CXCR2 axis in tumor microenvironment as potential diagnostic biomarker and therapeutic target. Cancer Commun (Lond) 2020; 40: 69-80.
[65] Gu Y, Feng Q, Liu H, Zhou Q, Hu A, Yamaguchi T, Xia S and Kobayashi H. Bioinformatic evi-

dences and analysis of putative biomarkers in pancreatic ductal adenocarcinoma. Heliyon 2019; 5: e02378.
[66] Zhang R, Liu Q, Peng J, Wang M, Li T, Liu J, Cui M, Zhang X, Gao X, Liao Q and Zhao Y. CXCL5 overexpression predicts a poor prognosis in pancreatic ductal adenocarcinoma and is correlated with immune cell infiltration. J Cancer 2020; 11: 2371-2381.
[67] Li A, King J, Moro A, Sugi MD, Dawson DW, Kaplan J, Li G, Lu X, Strieter RM, Burdick M, Go VL, Reber HA, Eibl G and Hines OJ. Overexpression of CXCL5 is associated with poor survival in patients with pancreatic cancer. Am J Pathol 2011; 178: 1340-1349.
[68] Wu B, Wang J, Wang X, Zhu M, Chen F, Shen Y and Zhong Z. CXCL5 expression in tumor tissues is associated with poor prognosis in patients with pancreatic cancer. Oncol Lett 2020; 20: 257.
[69] Aguirre AJ, Bardeesy N, Sinha M, Lopez L, Tuveson DA, Horner J, Redston MS and DePinho RA. Activated Kras and Ink4a/Arf deficiency cooperate to produce metastatic pancreatic ductal adenocarcinoma. Genes Dev 2003; 17: 3112-3126.
[70] Litman-Zawadzka A, Łukaszewicz-Zając M, Gryko M, Kulczyńska-Przybik A and Mroczko B. Serum chemokine CXCL8 as a better biomarker for diagnosis and prediction of pancreatic cancer than its specific receptor CXCR2, C-reactive protein, and classic tumor markers CA 19-9 and CEA. Pol Arch Intern Med 2018; 128: 524-531.
[71] Feng L, Qi Q, Wang P, Chen H, Chen Z, Meng Z and Liu L. Serum levels of IL-6, IL-8, and IL-10 are indicators of prognosis in pancreatic cancer. J Int Med Res 2018; 46: 5228-5236.
[72] Chen L, Fan J, Chen H, Meng Z, Chen Z, Wang P and Liu L. The IL-8/CXCR1 axis is associated with cancer stem cell-like properties and correlates with clinical prognosis in human pancreatic cancer cases. Sci Rep 2014; 4: 5911.
[73] Le X, Shi Q, Wang B, Xiong Q, Qian C, Peng Z, Li XC, Tang H, Abbruzzese JL and Xie K. Molecular regulation of constitutive expression of interleukin-8 in human pancreatic adenocarcinoma. J Interferon Cytokine Res 2000; 20: 935-946.
[74] Kuwada Y, Sasaki T, Morinaka K, Kitadai Y, Mukaida N and Chayama K. Potential involvement of IL-8 and its receptors in the invasiveness of pancreatic cancer cells. Int J Oncol 2003; 22: 765-771.
[75] O'Neill RS and Stoita A. Biomarkers in the diagnosis of pancreatic cancer: are we closer to finding the golden ticket? World J Gastroenterol 2021; 27: 4045-4087.
[76] Litman-Zawadzka A, Łukaszewicz-Zając M and Mroczko B. Novel potential biomarkers for pancreatic cancer-a systematic review. Adv Med Sci 2019; 64: 252-257.

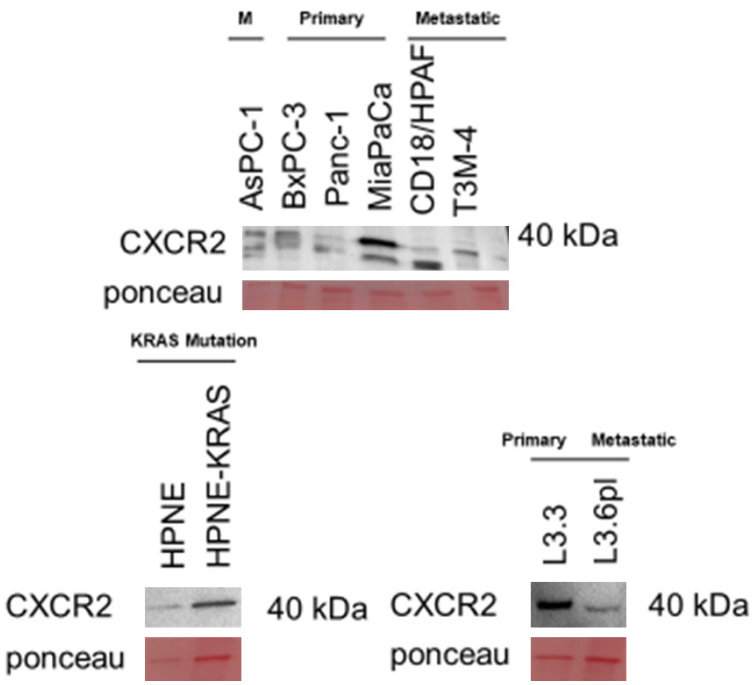

Supplementary Figure 1. Expression levels of CXCR2 proteins in the cell lysate of different PC cell lines: Western blot showing CXCR2 expression in cell lysates of different PC cell lines.

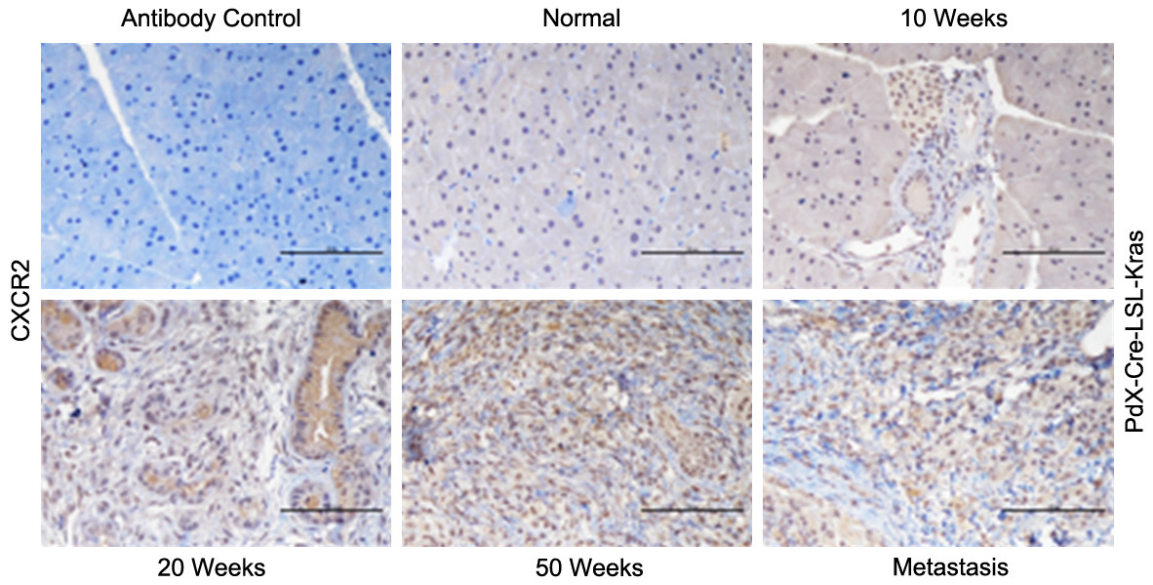

Supplementary Figure 2. Pathological expression of CXCR2 in PC progression model derived from tumors and metastasis of Pdx1-cre; LSL-Kras$^{(G12D)}$ (KC) mice. Representative images of CXCR2 IHC performed on a progression model derived from the normal pancreas (50-weeks), tumors at different ages (10-, 20-, and 50-weeks) and metastasis (liver, 50-weeks) of Pdx1-cre; LSL-Kras$^{(G12D)}$ (KC) mice (n=5). The pictorial graph demonstrates a progressive increase in qualitative CXCR2 expression in cancerous lesions of the KC mice model until 50-weeks with positive expression of these ligands in liver metastasis of 50-weeks mice. The normal pancreas of 50-week old Pdx1-cre mice was negative for CXCL1, CXCL3, and CXCL5 expression. The scale bar represents 100 mm.

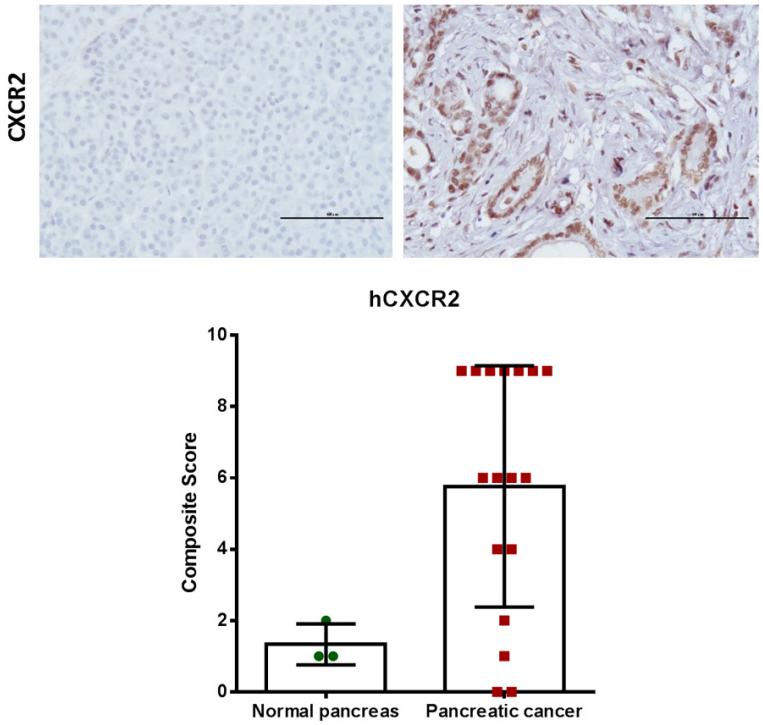

	Ducts	Other cells	Ducts	Stroma
CXCR2 +VE	0/3 (0%)	3/3 (100%)	10/12 (83.33%)	15/17 (88.235%)
CXCR2 -VE	3/3 (100%)	0/3 (0%)	2/12 (16.66%)	2/17 (11.76%)

Supplementary Figure 3. Pathological expression of CXCR2 receptor in PC patients. Representative images of CXCR2, IHC performed on the normal human pancreas and tumor tissue cores present in the TMA. Bar graph demonstrates quantitation of IHC score of CXCR2 staining in pancreatic tumor tissues. The scale bar represents 100 mm. The bar graph shows a high CXCR2 IHC score in the tumor in comparison with a normal pancreas.